

# UC Davis

## UC Davis Previously Published Works

### Title

Reach-scale bankfull channel types can exist independently of catchment hydrology

### Permalink

<https://escholarship.org/uc/item/6946k7qp>

### Authors

Byrne, Colin  
Pasternack, Gregory  
Guillon, Hervé  
et al.

### Publication Date

2019-11-04

### DOI

10.1002/essoar.10501068.1

Peer reviewed

# Reach-scale bankfull channel types can exist independently of catchment hydrology

*Colin F. Byrne<sup>1</sup>, Gregory B. Pasternack<sup>1</sup>, Hervé Guillon<sup>1</sup>, Belize A. Lane<sup>2</sup>, Samuel Sandoval-Solis<sup>1</sup>*

<sup>1</sup>University of California Davis, Department of Land, Air & Water Resources

<sup>2</sup>Utah State University, Civil and Environmental Engineering

## Citation

This document is a reprint of a paper accepted for publication in *Earth Surface Processes and Landforms*. It can be cited as follows:

Byrne CF, Pasternack GB, Guillon H, Lane BA, Sandoval-Solis S. 2020. Reach-scale bankfull channel types can exist independently of catchment hydrology. *Earth Surface Processes and Landforms*. <https://onlinelibrary.wiley.com/doi/10.1002/esp.4874>

## Abstract

Reach-scale morphological channel classifications are underpinned by the theory that each channel type is related to an assemblage of reach- and catchment-scale hydrologic, topographic, and sediment supply drivers. However, the relative importance of each driver on reach morphology is unclear, as is the possibility that different driver assemblages yield the same reach morphology. Reach-scale classifications have never needed to be predicated on hydrology, yet hydrology controls discharge and thus sediment transport capacity. The scientific question is: do two or more regions with quantifiable differences in hydrologic setting end up with different reach-scale channel types, or do channel types transcend hydrologic setting because hydrologic setting is not a dominant control at the reach scale? This study answered this question by isolating hydrologic metrics as potential dominant controls of channel type. Three steps were applied in a large test basin with diverse hydrologic settings (Sacramento River, California) to: (1) create a reach-scale channel classification based on local site surveys, (2) categorize sites by flood magnitude, dimensionless flood magnitude, and annual hydrologic regime type, and (3) statistically analyze two hydrogeomorphic linkages. Statistical tests assessed the spatial distribution of channel types and the dependence of channel type morphological attributes by hydrologic setting. Results yielded ten channel types. Nearly all types existed across all hydrologic settings, which is perhaps a surprising development for hydrogeomorphology. Downstream hydraulic geometry relationships were statistically significant. In addition, cobble-dominated uniform streams showed a consistent inverse relationship between slope and dimensionless flood magnitude, an indication of dynamic equilibrium between transport capacity and sediment supply. However, most morphological attributes showed no sorting by hydrologic setting. This study suggests that median hydraulic geometry relations persist across basins and within channel types, but hydrologic influence on geomorphic variability is likely due to local influences rather than catchment-scale drivers.

Keywords: channel-reach morphology, multivariate classification, hydrogeomorphic, hydraulic geometry, basin hydrology

## Introduction

### The importance of reach-scale morphological classification

Classification of reach-scale morphology is fundamental for integrated river basin management to organize understanding of river forms, process dynamics, and physical habitat along the river network (Gurnell et al., 2016; Kondolf et al., 2016). Numerous river restoration and management protocols leverage reach-scale classifications in a variety of settings throughout the world (Brierley and Fryirs, 2000; Kondolf et al., 2016; Paustian, 2010; Poff et al., 2010; Schmitt et al., 2007). In particular, reach-scale morphology and associated processes are indicative of specific hydraulic conditions (Lane et al., 2018a) that can control biogeochemical and ecological functioning for aquatic species (Dahm et al., 1998; Moir and Pasternack, 2010). Here, we use the term reach-scale morphology to describe streams with similar valley, cross-sectional, planform, longitudinal bedform, and sediment characteristics at scales of 10 – 20 channel widths, or more simply, streams comprised of similar morphological units in similar valley settings (Frissell et al., 1986; Wyrick and Pasternack, 2014).

Reach-scale classifications seek to organize complex morphologies and processes occurring across a landscape. Although classifications have been conducted for a variety of purposes (see Kondolf et al., 2016 for review), reach-scale morphology represents a mesoscale in which smaller geomorphic units are integrated and larger channel segment and basin processes must be represented by a given smaller form (Frissell et al., 1986). Reach-scale classifications can focus on measured channel attributes and capture sub-reach scale morphological features and hydraulic conditions, such as pool formation by flow-convergence routing or secondary flow dynamics (MacWilliams et al., 2006; Thompson, 1986). Other classifications apply a simplified process domain concept focusing on a metric of erosive force across scales and attempt to correlate reach-scale morphology with reach-, segment-, or basin-scale processes using remotely-sensed channel slope, valley confinement, and drainage area (Church, 2002; Flores et al., 2006; Montgomery, 1999; Polvi et al., 2011; Wohl, 2010).

Classifications are static representations of dynamic systems driven by hydrologic and geomorphic processes influencing reach-scale morphology across multiple scales (Lane, 1995). Although reach-scale morphology (e.g. step-pool, riffle-pool) may remain stable through time, sub-reach scale characteristics exist within an erosional or depositional cycle and are subject to both gradual and nearly instantaneous complex changes (Schumm, 1977). Even within the same reach, entrainment of a given sediment clast can occur under flow conditions ranging from well below flood stage to the rarest flood events (Miller et al., 1977; Shields, 1936). Because entrainment may occur over a range of hydrologic disturbance magnitudes, a relationship may develop between these disturbances and a classified morphology. Given two reaches with similar basin-scale geomorphic settings and sediment size distributions, do differences in reach-scale morphology and channel attributes exist in streams with different patterns or magnitudes of hydrologic disturbance? Alternatively, do two streams exhibit differences in sediment characteristics and morphology because of differences in hydrologic disturbance?

## The untested influence of hydrology on reach-scale morphology

While reach-scale morphology is thought to be driven by catchment hydrology, sediment delivery, and topography, the relative influence of these controls is often unclear. Attempts to relate reach-scale morphology to local hydrology and streamflow patterns stem from established fundamental downstream relationships between discharge magnitude and channel hydraulic geometry (Leopold and Maddock, 1953; Richards, 1977). Bankfull discharge has been combined with slope to represent both hydrologic and landscape influences on transport capacity when defining channel planform (Leopold and Wolman, 1957). Leopold and Wolman (1957) noted the related nature of channel cross-section geometry, planform, longitudinal form, and sediment characteristics. A reach-scale classification aims to encapsulate all of these dimensions of form, which clearly infers inclusion of a discharge metric in classification methodologies.

Hydrologic variables such as channel forming flow, flood magnitude, and contributing area are fundamental to many process domain classifications and analyses (Church, 2002; Flores et al., 2006; Polvi et al., 2011). These classifications have better predictive power when a hydrologic-based metric representative of transport capacity is included (Flores et al., 2006), as compared to previous slope-based classifications established by Grant et al. (1990) and Montgomery and Buffington (1997). However, the use of discharge-slope thresholds to define river pattern has been challenged, and evidence suggests that channel geometry, planform, and reach-scale morphology are more closely related to sediment supply and grain size characteristics (Carson, 1984; Church, 2006; Friend, 1993; Harvey, 1991; Pfeiffer et al., 2017). It is not surprising that both hydrology and sediment supply are controls on reach-scale morphology, but to what degree is unclear. If transport capacity is indeed the primary driver of channel form, channel types should reflect the hydrologic setting in which a reach exists.

Hydrologic setting is defined here as the reach-scale hydrologic conditions represented by the following metrics: flood magnitude, dimensionless flood magnitude, or annual hydrologic regime. We define the annual hydrologic regime as the characteristic patterns of streamflow (e.g., magnitude, frequency, duration, rate of change, and timing) at any location over a year (Poff et al., 1997). To simplify these patterns, hydrologic regimes are often classified into groups of sites with similar streamflow patterns (Bard et al., 2015; Beechie et al., 2006; Lane et al., 2017a; Thanapakpawin et al., 2007; Yang et al., 2002).

In contrast with the literature linking channel metrics to local discharge or transport capacity metrics, no studies have demonstrated a link between channel metrics and annual hydrologic regimes within a region. Pfeiffer and Finnegan (2018) note that continental differences in the mobilization of gravel-bed stream sediments, fundamental to the formation of bedforms, occur first due to sediment supply and second due to differences in hydrologic regime. Whether these findings result in distinct reach-scale morphologies is unknown. In a more dichotomous comparison of hydrologic differences in channel form, arid and humid landscapes exhibit differences in channel attributes and sensitivity to hydrologic disturbances (Graf, 1988; Reid and Laronne, 1995; Tooth, 2000). At a regional scale, it is unclear whether differences in flow timing, duration, or volume associated with hydrologic disturbances of a snowmelt-dominated regime would yield different reach-scale channel types than disturbances governed by a rain-dominated regime. For example, a rain-dominated system may be subject to flashier high flow events while a snowmelt system may exhibit longer duration flood events. Therefore, it is worth investigating if channel type differences, which exist in regions with extreme differences in hydrologic disturbance, also exist within regions with smaller differences in hydrologic disturbance.

Despite some support in the literature for dominant hydrologic setting control on reach-scale morphology, complexity in local channel type formation complicates these relationships. Bedrock, large wood, vegetation, and bioengineered structures can influence reach-scale morphology by forcing the occurrence of certain morphological units (Bisson et al., 1996; Buffington et al., 2002; Fryirs and Brierley, 2012; Montgomery et al., 1996; Wohl, 2013). If a reach is continually subjected to these biological and geological influences, the hydrologic setting is less likely to determine reach-scale morphology. Whether or not hydrologic setting exerts dominant control over local processes is unclear.

In addition to complexity exerted by local geomorphic influences, there is ample evidence that similar morphologies can exist across a range of arid to humid hydrologic settings (Chin and Wohl, 2005; Makaske, 2001; Montgomery and Buffington, 1997; Sutfin et al., 2014). An argument for limited hydrologic control on reach-scale morphology may be inferred from Hack (1960), who postulated that rivers have many mutually adjustable variables operating via many mechanisms of fluvial adjustment. A shift or difference in hydrologic setting may simply be adjusted away by something else, such as topographic controls or biological influences, without necessitating a shift or difference in channel type. Alternatively, reach-scale morphology could be explained by the minimum energy principle. In this case, a difference in hydrologic setting may not change the fundamental need for a particular reach-scale morphology to be present in order to satisfy a number of documented extremal conditions such as minimum hydraulic dimension variance, minimum energy dissipation rate, minimum stream power, or maximum friction factor (Chang, 1979; Davies and Sutherland, 1983; Huang et al., 2004; Langbein and Leopold, 1964; Yang et al., 1981).

To provide more complete understanding of reach-scale morphological controls, we explicitly investigate the relationship between hydrologic setting and reach-scale morphology within a river basin through an array of statistical methods. In particular, we aim to answer the following open scientific question: is hydrologic setting a dominant control on reach-scale morphology, or is morphology largely independent of hydrologic setting because other topographic and local characteristics exert stronger controls? The experimental design for addressing this question is below (Section 2), followed by specific methodologies in Sections 4 through 6.

## Experimental design

In this study, we quantitatively investigated the relationship between reach-scale morphology and hydrologic setting using several statistical methods. Geomorphic metrics representing reach-scale morphology include common field-measured channel attributes (e.g., bankfull depth) and categorically classified morphologies (e.g., pool-riffle), henceforth called channel types. Both reach-scale channel attributes and channel types were determined from field surveys. Hydrologic setting is quantified as the specific value of one of three hydrologic metrics: flood magnitude, dimensionless flood magnitude, or gauge-extrapolated annual hydrologic regime (represented by a classification system derived in Lane et al. 2017a and 2018a). Annual hydrologic regime type is already a set of discrete identifiers, whereas flood magnitude metrics are continuous variables that first need to be binned into categories to make all three metrics comparable.

The three categorized hydrologic metrics were analyzed in conjunction with reach-scale morphology to answer two specific hydrogeomorphic questions: (1) do reach-scale channel types exist independently of hydrologic setting, and (2) do reach-scale channel attributes of a given channel type show statistical differences between hydrologic settings? Statistical bootstrapping and nonparametric

Kruskal-Wallis tests were used to quantitatively assess the hydrologic-geomorphic relationships for questions (1) and (2), respectively. Given categorized hydrologic metrics and reach-scale channel types, a channel type occurring across all hydrologic metric categories indicates no hydrologic setting control on channel type occurrence (Fig. 1-a1). A channel type occurring in a single hydrologic metric category indicates hydrologic setting control (Fig. 1-a2). In terms of field-measured channel attributes, no significant difference between hydrologic metric categories indicates no hydrologic setting control on the channel attribute (Fig. 1-b1). A significant difference between hydrologic metric categories indicates hydrologic setting control on the channel attribute (Fig. 1-b2). The experimental design is conceptualized in Figure 1, the test basin is presented in Section 3 and the specific methodologies related to reach-scale morphology, reach-scale hydrologic setting, and statistical testing of hydrogeomorphic relationships are explained in Sections 4, 5, and 6, respectively.

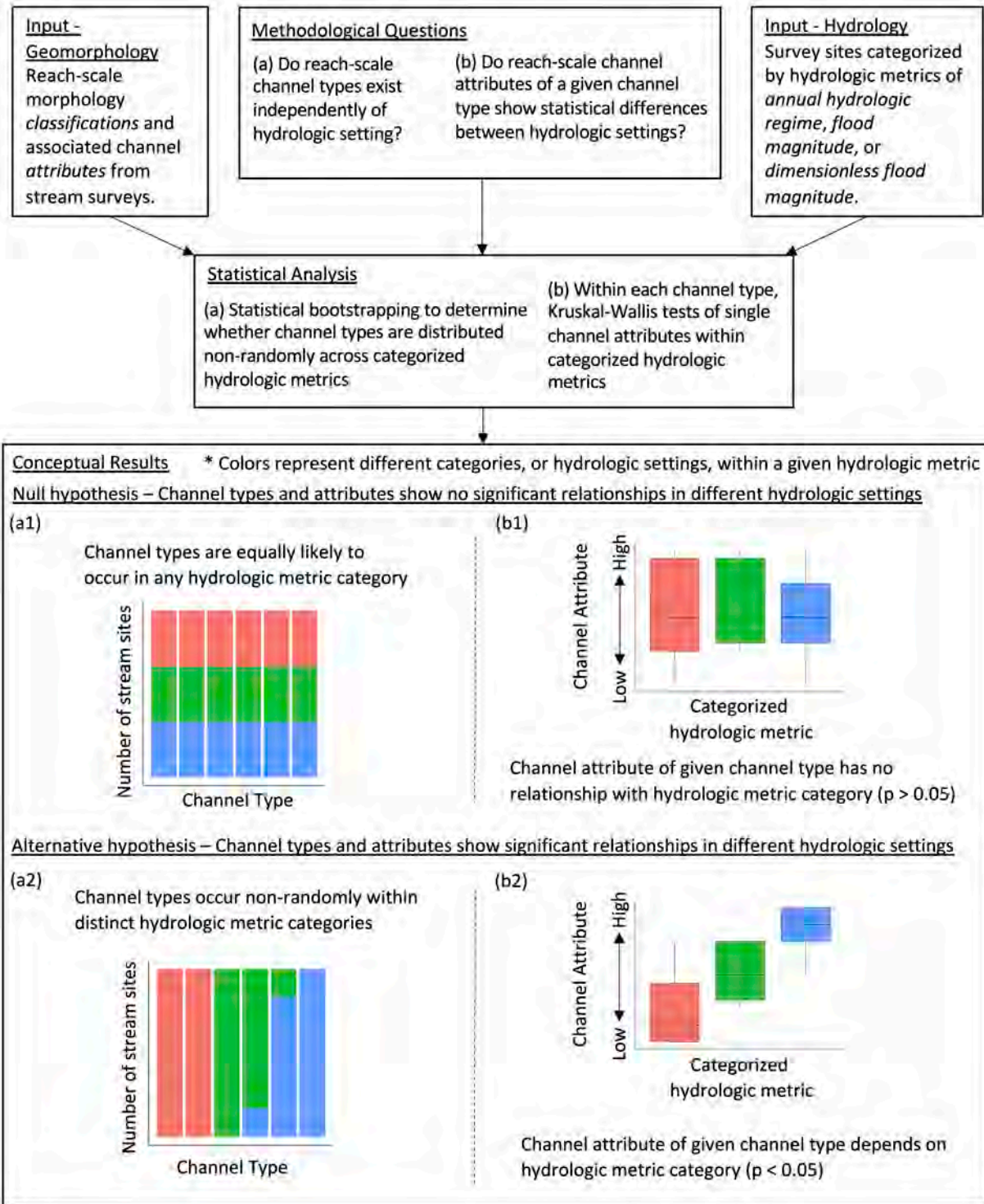


Figure 1. Conceptual diagram representing the experimental design used in this study. In the results box, graphics (a1) and (b1) illustrate the possible outcome in which hydrologic setting has no explanatory power to differentiate among any channel types or any channel attributes. In graphics (a2) and (b2), hydrologic setting is envisioned to have dominant explanatory power over channel types.

## Test basin

The Sacramento River basin is the second largest river by volume draining to the Pacific Ocean in the continental United States, making it suitably large and hydrogeomorphically diverse to serve as the testbed for this study (Palmer, 2012). The basin covers approximately 70,000 km<sup>2</sup>, predominantly within California with the northernmost headwaters extending into Oregon (Fig. 2). The Sacramento River basin is comparable to the Yodo (Japan), Kizilirmak (Turkey), and Seine (France) rivers, and estimated to be one of the largest 200 rivers draining directly to an ocean (Milliman and Syvitski, 1992). The basin is geologically complex with multiple physiographic provinces including the Coastal range to the west, the southern Cascade Range, the Sierra Nevada, the volcanic uplands of the Modoc Plateau, and the basin and range province in northeastern California. The Sacramento River flows roughly north to south through the Central Valley of California and combines with the San Joaquin River to form the Sacramento-San Joaquin River Delta, which ultimately drains into the Pacific Ocean through the San Francisco Bay.



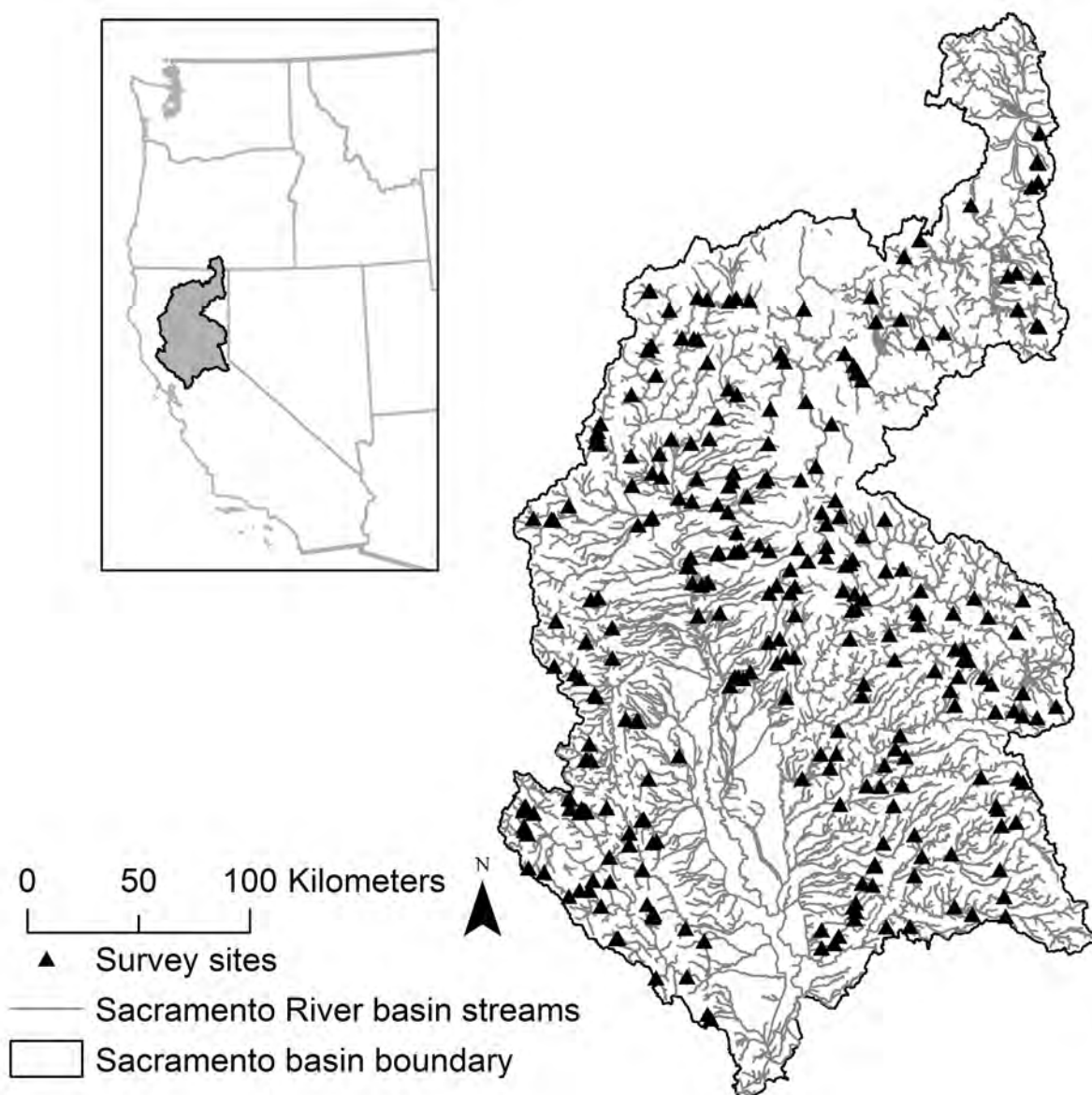


Figure 2. Map of the Sacramento River basin showing 288 stream survey locations among 2nd order and larger streams.

The Sacramento River basin exhibits order-of-magnitude differences in mean annual precipitation, with approximately 28 cm in the northeastern high plateau and basin and range settings to over 275 cm in the northern Sierra Nevada (PRISM Climate Group, 2007). The basin is subjected to a Mediterranean climate with cool, wet winters and warm, dry summers. The seasonality and inter-annual variability of storm events plays a large role in the spatiotemporal distribution of flow regimes across the state, while topographic and geologic variabilities add further complexity. Within the basin, portions of the Coastal Range and Sierra Nevada can be subjected to similar major winter storm events, but differences in elevation and topographic orientation drive strong differences in annual hydrologic regime (Lane et al., 2017a).

In addition to the complex physiographic and climatic conditions across the basin, streams within the Sacramento River basin have been subjected to a plethora of human-induced hydrogeomorphic alterations over the past two hundred years. Perhaps the most well documented and glaring human-induced fluvial changes were due to hydraulic mining within the basin, of which the impacts are ongoing (Gilbert, 1917; James, 1991; White et al., 2010). Hydrologically, at least 435 dams are in the basin, which will impact the hydrogeomorphology of the streams locally, at the very least, and in some cases have lingering impacts to the entire basin (Kondolf, 1997; Singer, 2007). Heavy agricultural and urban development dominates the Central Valley, and other land use practices include but are not limited to logging, gravel pit mining, and animal grazing (Mount, 1995). All of these changes are important to keep in mind when examining hydrogeomorphic relationships throughout the basin and are addressed in more detail in Section 4.1 in relation to sites analyzed in this study.

## Classification of reach-scale morphology

Our quantitative investigation of hydrogeomorphic relationships requires defining measurable geomorphic metrics representing reach-scale morphology. This section presents methods used both to estimate commonly used reach-scale geomorphic attributes and to derive a novel channel type classification.

A multivariate data-driven statistical approach to reach-scale classification was used in this study to avoid preconceived channel type descriptions and is similar to other statistical classifications (e.g. Sutfin et al. (2014) or Kasprak et al. (2016)). Twelve geomorphic attributes were considered for the reach-scale classification. Nine geomorphic attributes were calculated from field surveys: water surface slope ( $s$ ), bankfull depth ( $d$ ), bankfull width ( $w$ ), bankfull width-to-depth ratio ( $w/d$ ), coefficient of variation of bankfull depth ( $CV_d$ ), coefficient of variation of bankfull width ( $CV_w$ ), median grain size ( $D_{50}$ ), 84th percentile grain size ( $D_{84}$ ), and channel roughness ( $d/D_{50}$ ). Three additional geomorphic attributes were estimated using geographic information system (GIS) techniques: hydrologic contributing area ( $A_c$ ), sinuosity ( $k$ ), valley confinement distance ( $C_v$ ).

### Site selection

A stratified statistical sampling design selected a reasonable number of representative sites to characterize variability in fluvial geomorphic settings across the landscape. Out of approximately 119,000 possible 200-m reaches basin-wide, a total of 288 wadeable stream reaches were selected for surveying with 139 and 149 surveyed by the University of California Davis (UCD) and by the California State Water Resources Board's Surface Water Ambient Monitoring Program (SWAMP), respectively (Fig. 2). Because the study focused on wadeable streams of 2nd or larger Strahler-order, over 90% of survey sites were on 2nd to 4th order streams (Strahler, 1957). In addition, over 90% of sites were located in one of the six mountainous Level III ecoregions that make up the basin (Omernik, 1987). Survey sites were selected to avoid confluence influences with median distances of 431 meters and 43 bankfull channel widths away from the nearest confluence.

A geospatial analysis selected specific survey locations using a ESRI ArcGIS 10.4 (ESRI, 2016). Contributing area was calculated based on the United States Geological Survey (USGS) 10-m National Elevation Dataset (NED) and streamlines defined by the National Hydrography Dataset (NHD) version 2 (Gesch et al., 2002; McKay et al., 2012). Slope was estimated from the 10-m DEM

as the change in elevation along the reach divided by the reach length. Because desktop estimates of slope are susceptible to error, especially for short stream segments (Neeson et al., 2008), slope was re-calculated from survey measurements for use in subsequent geomorphic statistical analysis. GIS desktop slope computation was not used in the geomorphic classification and only aided site selection.

Field survey site locations were determined using an equal effort stratified random sampling scheme based on GIS-desktop-computed slope and contributing area values, as documented in Lane et al. (2017b). Slope categories, based on Rosgen (1994) as a classification comparison, were defined as <0.1%, 0.1-2%, 2-4%, 4-10%, and >10%. Contributing area categories differed based on physiographic province (i.e. Pacific Border or Cascade-Sierra Nevada) due to the assumption that differences in climate, topography, and lithology would drive differences in transport capacity under similar contributing area settings (Lane et al., 2017b). Pacific Border area categories were <50, 50-5,000, and >5,000 km<sup>2</sup>, while Cascade-Sierra Nevada sites were <300, 300-9,000, and >9,000 km<sup>2</sup>. The slope - area sampling protocol was designed to capture variability in transport capacity. Since some slope - area bins were expected to be more prevalent on the landscape than others (e.g. streams of a given Strahler order are approximately twice as common as streams of one higher order), an equal number of reaches was surveyed in each bin to ensure that all channel settings, including rare channel types, are represented in the classification.

In relation to anthropogenic impacts within the basin, 88% of the sites surveyed in this study are classified as free flowing rivers (Grill et al., 2019), although impacts to low order streams may not always be appropriately represented in this number (Grill et al., 2019). The numerous stream reaches in the basin with large upstream storage dams that have been documented to substantially alter hydrology were not the focus of this study (Singer, 2007). The land use of survey sites can be summarized as 70% forest and woodland, 13% developed and other human use, 10% shrub and herb vegetation, 5% agricultural and developed vegetation, and 3% desert and semi-desert (USGS, 2016). Of the developed sites, 76% exist within open space while the remaining 24% exist in low or medium development (USGS, 2016). Sites that showed clear evidence of human engineering along the survey length were not included in this analysis. As the majority of these sites exist within mountainous, forested sites, we expect that mining, logging, or grazing would impose the most relevant hydrogeomorphic changes to these sites. However, there has been ample time (e.g., decades) and sufficient flooding for Hack's (1960) "quick" natural geomorphic adjustments to such anthropogenic impacts. In addition, sediment yields within the basin have fallen considerably since the peak of hydraulic mining (Wright and Schoellhamer, 2004). This means that if an overarching hydrologic setting control on channel type exists, it should be able to readjust such mountain-setting anthropogenic dynamics and be clearly apparent in the data. Selecting sites with a stratified sampling approach ideally normalizes the anthropogenic impacts across all sites.

## **Site data acquisition and processing before classification**

Field surveys were completed by UCD survey teams in summers of 2015 through 2017. Survey methodologies were based on SWAMP protocols to enable comparability between datasets (Ode, 2007). At each site, average bankfull width was estimated to determine the reach survey length. Survey lengths were 150 or 250 m for streams with average wetted widths less than or greater than 10 m, respectively, as is required in the SWAMP protocol. This produced stream reaches with a median length of 18.8 channel widths. Eleven equally spaced cross-sectional transects along the reach were surveyed using rod and level techniques. Bankfull depth was defined using geomorphic

and vegetative indices as defined by Ode (2007) for SWAMP protocols, including slope breaks, change from annual to perennial vegetation, and changes in sediment size. Bankfull depth and water depth were recorded at the thalweg. A Wolman pebble count was conducted at each transect (Wolman, 1954), and a longitudinal survey was conducted along the thalweg at each cross-section.

Mean values of bankfull width, depth, and bankfull width-to-depth ratio were calculated as the mean of all survey transect measurements. In addition, 50th and 84th percentile grain sizes were calculated over the entirety of each reach. If the channel was split within the survey length, bankfull depth was calculated as the mean of each split channel at a given transect and bankfull width was calculated as the sum of each split channel width. Width-to-depth of split channels at a transect was calculated as the average width-to-depth of each individual channel. Reach slope was calculated from the best-fit regression line of surveyed water surface elevations along the thalweg. The roughness parameter was calculated as the ratio of bankfull depth to median grain size. Within-reach coefficients of variation of bankfull width and bankfull depth were calculated as the ratio of standard deviation to mean attribute values across the surveyed transects. Here, coefficients of variation of width and depth are referred to as topographic variability attributes (TVAs), which can exhibit considerable importance in identifying distinct channel types (Lane et al., 2017b).

A GIS was also used to estimate certain channel and valley attributes used in statistical analysis: contributing area, sinuosity and valley confinement. The same values of contributing area used in site selection were used in site classification (see Section 4.1). Sinuosity has been used as a defining metric in previous classifications (Rosgen, 1994) and was calculated as the ratio of channel thalweg length to distance between upstream and downstream vertices. Stream channels were digitized based upon aerial imagery, digital USGS topographic maps, and NHD layers for 1000 m. Because sinuosity is sensitive to the scale at which it is calculated (Snow, 1989), 1000 m sinuosity was used to represent the channel reach length at approximately 100 times the bankfull width, which would capture channel meandering at sites with both small and large channels.

Valley confinement and setting play both qualitative and quantitative roles in the majority of previous channel classification methodologies due to the influence of distinct valley setting processes in the creation of characteristic forms (Beechie and Imaki, 2014; Brierley and Fryirs, 2000; Fryirs et al., 2016; O'Brien et al., 2019; Rosgen, 1994). Here, valley widths were delineated using a methodology similar to previous literature (Gilbert et al., 2016; O'Brien et al., 2019). For the purposes of this study, 25 percent slope was chosen as a threshold between valley bottom and valley wall capturing a medial value between clay and sand dominated hill footslopes (Carson, 1972). The 10-m DEM was converted to a slope raster to create valley bottom polygons of less than 25% slope. Cross-sections of 5,000 m, a distance great enough to decipher between small upland and large lowland valleys, were reduced in length so that the cross-sections spanned the local channel-bounding valley bottom polygon. Four cross-sections per 200-m of stream length were averaged to calculate a single valley confinement distance that was subsequently used in the geomorphic classification. Confined, partly-confined, and unconfined valley nomenclature of channel type valley setting was defined by a logarithmic scale of  $\leq 100$  m,  $>100$  and  $\leq 1000$  m, and  $> 1000$  m, respectively.

## **Multivariate statistical channel archetyping**

Our multivariate statistical reach-scale classification used a similar method as Lane et al. (2017b) and followed five general steps: (1) data preparation, (2) informative analysis of multivariate distances and variance between survey sites, (3) classification of sites, (4) classification validation,

and (5) quantification of channel types. The R language was used for all analysis (R Core Team, 2017). Data preparation consisted of rescaling reach-scale attributes from zero to one and removing highly correlated attributes based on Pearson correlation (correlations  $> 0.7$  or  $< -0.7$ ). Methods and results for step two are presented in Supplementary Information since they are less directly relevant to answering the specific research question addressed herein (Supplementary Information Figs. S3 & S4).

Site classification was conducted using Ward's algorithm (Ward's hierarchical clustering; WHC) (Murtagh and Legendre, 2014a, 2014b; Ward, 1963) and complemented with heuristic refinement. The WHC utilized the 'hclust' function with the 'Ward.D2' (stats package) and the 'NbClust' function to assess the suggested number of hierarchical clusters using the graphical Hubert and Arabie index (NbClust package) (Hubert and Arabie, 1985; Murtagh and Legendre, 2014a). The WHC minimizes within-cluster variance and maximizes between-cluster variance. The variance between sites was based on Euclidean distances. Here, heuristic refinement is based on expert opinion and refers to an iterative process of examining site photographs and interpreting geomorphic context of each site and its defining channel type. This process assesses whether statistical branches are indeed representative of differences in reach-scale form or are the result of multivariate distances between sites that may accumulate but are not representative of obvious form characteristics in comparison with other channel types. The goal of heuristic refinement was not to make large adjustments to the purely statistical classification, but to ensure that it was capturing real-world differences.

The validation step used the 'rpart' package to calculate classification tree performance in correctly binning channel types and assessing cross-validation accuracy (De'ath and Fabricius, 2000; Therneau and Atkinson, 2018). Classification trees represent a diagnostic tool and interpretable technique to understand the stability of the multivariate clustering. Cross-validation accuracy is a measure of the model to generalize to unseen data. Finally, pair-wise significant differences between channel types were quantified using Dunn Tests with the 'dunn\_test' function (rstatix package) (Kassambara, 2019).

Steps three through five were iteratively repeated. A combination of reach-scale attributes was used as input to the final three steps. For example, in the first iteration, only reach-scale attributes that were not highly correlated were considered. If the input attributes led to low classification tree cross-validation performance or a low number of pair-wise significant differences between channel types, a different combination of input attributes was tested. Ultimately, the combination that produced the highest cross-validation percentage was retained for the final classification.

## **Hydrologic metric categorization methods to assess hydrogeomorphic questions**

This section describes categorization of the three hydrologic metrics considered in this study as alternative representations of hydrologic setting.

### **Flood magnitude**

Flood peak magnitude was used to assess the strength and capability of hydrologic disturbance to carve a river of any specific type. Theoretically, small floods should not be able to create the

same channel types are large floods. Sacramento River basin flood magnitudes were collected from a previous USGS flood-frequency analysis of gauges with a minimum of 30 years of unregulated flow (Parrett et al., 2011). Only gauges located along streamlines described by the hydrologic classification of five annual hydrologic regimes were used for a total of 84 locations with USGS flood-frequency estimates. Statistically significant contributing area-discharge regressions were generated for each of the annual hydrologic regimes based on gauge records (see Supplementary Information Fig. S2, Table S3). Flood magnitudes of 2-, 5-, 10-, 25-, and 50-year recurrence intervals were calculated from the regressions at each of the channel survey sites. A proportional flood magnitude metric of the ratio of Q50-year to Q2-year was also investigated. Ultimately, 10-year recurrence interval floods were considered here because, under this condition, statistically significant results presented in this study were most consistently maximized. Use of the results that maximized statistically significant returns would provide the strongest indication of hydrologic setting influence on reach-scale morphology. The 10-year recurrence interval has physical importance because California has experienced an approximately decadal flood recurrence interval over its measured and longer anecdotally recorded history (Dettinger, 2016; Guinn, 1890). Such a consistent disturbance regime would be expected to influence channel type if hydrologic setting is indeed a dominant control.

Site-specific flood magnitudes were linearly binned into terciles (<33%, 33-66%, >66%), to represent low, medium, and high flood magnitudes, respectively (Fig. 3a). In addition, a decile linear binning was done to equal the number of channel types. Tercile categories are more appropriate for determining statistical significance between low and high flood magnitudes while decile categories are more appropriate for determining whether channel types exist in significantly few flood magnitude categories.

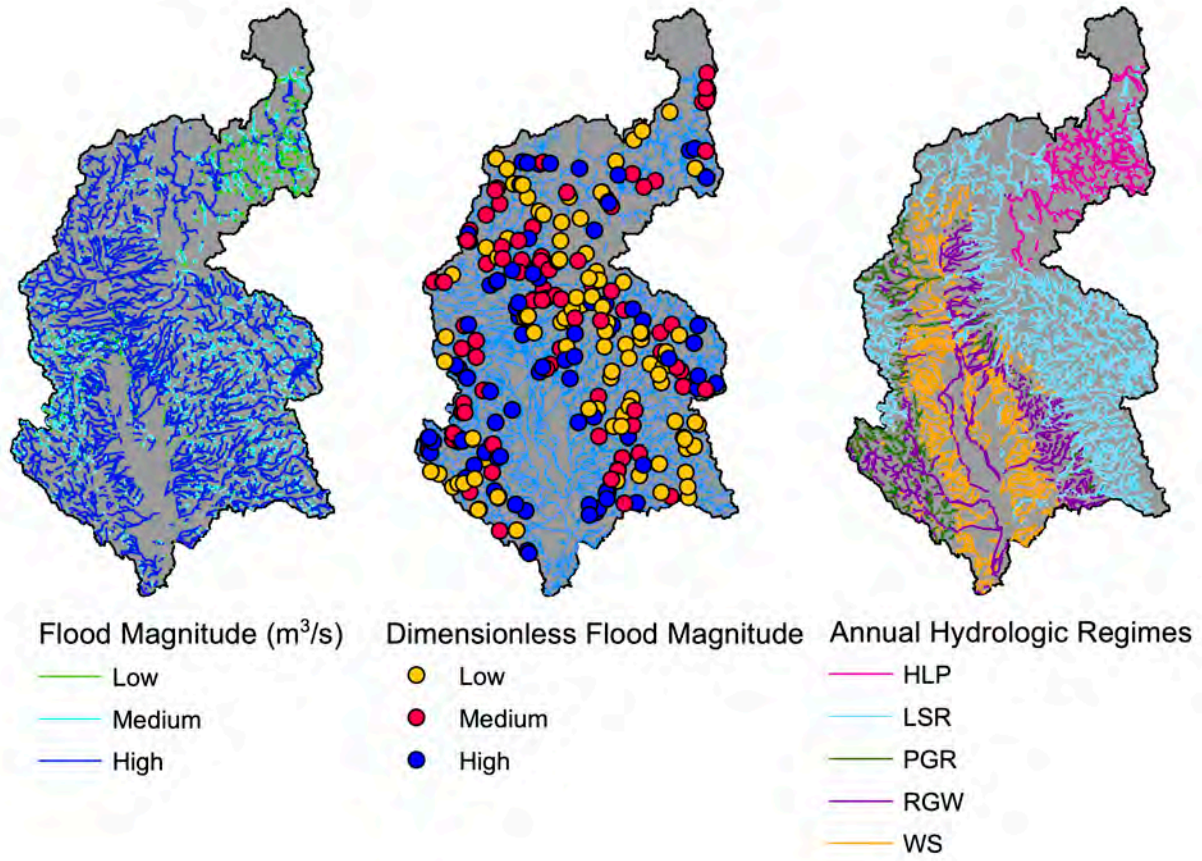


Figure 3. Hydrologic settings binned by stream length for (a) flood magnitude (adapted from Parrett et al. 2011) (b) by site for dimensionless flood magnitude, and (c) by stream length for annual hydrologic regime (derived from Lane et al, 2018b).

### Dimensionless flood magnitude

Because a given flood magnitude is expected to have different impacts in channels of varying geometry and grain size, flood magnitude was scaled by geomorphic attributes to ascertain a dimensionless relative disturbance value. Dimensionless flood magnitudes were calculated by non-dimensionalizing discharges calculated in the flood magnitude analysis by median grain size ( $D_{50}$ ) and bankfull width ( $w$ ). Dimensionless discharge was previously defined by Parker (1979) and Pitlick and Cress (2002) (Eqn. 1).

$$\tilde{Q} = Q/(\sqrt{RgD_{50}} * D_{50}^2) \text{ (Eqn. 1)}$$

Here  $R$  is the submerged specific gravity of sediment assumed to be 1.65 and  $g$  is the acceleration due to gravity. The equation was adapted for this study to account for channel dimensions (bankfull width,  $w$ ) in addition to  $D_{50}$  with the interest of understanding the relative magnitude of a defining flood in relation to channel dimensions and roughness elements (Eqn. 2).

$$\tilde{Q} = Q/(\sqrt{RgD_{50}} * w^2) \text{ (Eqn. 2)}$$

Similar to dimensional flood magnitudes, sites were grouped into low, medium, or high dimensionless flood magnitude using terciles (Fig. 3b), and split into ten quantile categories.

## Annual Hydrologic Regime

A previously established hydrologic stream classification within California defines key characteristics of the dominant annual flood hydrograph related to timing, magnitude, duration, frequency, and rate of change characteristics at a given location (Lane et al., 2018b). Lane et al. (2018b) classified stream gauges in California based on a variety of hydrologic indices (e.g. mean annual flow, date of minimum/maximum flow, small/large flood frequency, etc.) and extrapolated those attributes using topographic, geologic, and climatic conditions to define annual hydrologic regimes to ungauged streams (Lane et al., 2017a). Annual hydrologic regime types were directly attributed to reach-scale survey sites in this study using the NHD stream network.

Five annual hydrologic regimes were represented by the 288 surveyed channel reach locations included High elevation and Low Precipitation (HLP) (n = 25), Low-volume Snowmelt and Rain (LSR) (n = 120), Perennial Groundwater and Rain (PGR) (n = 54), Rain and seasonal Groundwater (RGW) (n = 51), and Winter Storms (WS) (n = 38) (Table 1, Fig. 3c). Differences captured by these annual hydrologic regimes may theoretically result in differences in channel form. For example, HLP streams may be subjected to lower specific water yields than PGR streams, which may result in transport of relatively smaller grain sizes. The WS streams may exhibit differences in flashiness compared to LSR streams which could result in differences in the duration of sediment transport. Finally, rainfall events in RGW and PGR streams may alter channel form differently based on differences in groundwater contributions and runoff and erosion characteristics of corresponding catchments.



Table 1. Description of annual hydrologic regimes within the Sacramento River Basin (Adapted from Lane et al. (2017a, 2018b)).

Class	Hydrologic Classification	Hydrologic Characteristics	Physical and Climatic Catchment Controls
HLP (25 sites)	High elevation, low precipitation	Upland streams with low discharge, but a distinct snowmelt pulse	Catchments predominantly located on the Modoc Plateau with high elevations and dominated by volcanic rock and high organic content soils
LSR (120 sites)	Low-volume snowmelt and rain	Transition between snowmelt and high-volume snowmelt and rain AND bimodal with distinct spring snowmelt pulse and winter rain peaks	Mid-elevation catchments with limited contributing areas and low winter temperatures
PGR (54 sites)	Perennial groundwater and rain	Characteristics of winter storms (predictable winter rain events) and groundwater (low seasonality), but generally stable flows	Low elevation catchments with low riparian soils clay content or underlain by residual sedimentary rock materials
RGW (51 sites)	Rain and seasonal groundwater	Bimodal hydrograph driven by predictable winter rains and supplemented at other times by groundwater	Low elevation catchments with limited winter precipitation often associated with igneous and metamorphic rock materials OR Coastal catchments with small aquifers driving short residence times
WS (38 sites)	Winter storms	Predictable large fall and winter rainfall with January peak flows	Low elevation catchments with substantial winter precipitation

## Methods to assess dominant hydrologic influence on reach-scale morphology

Prior to statistical analysis of hydrologic setting influence on channel type, multivariate outliers within each channel type were removed. Multivariate outliers suggest forms that differ from the median tendencies of a multivariate cluster, making them least representative of a given channel type and less indicative of relationships between that channel type and hydrologic setting. Mahalanobis distances were used to determine multivariate outliers based on the ‘mvoutlier’ package (Filzmoser et al., 2005; Filzmoser and Gschwandtner, 2012) with the chi-squared quantile specified as 97.5% and a proportion of observations used in calculation of the minimum covariance determinant of 0.75.

To address the hydrogeomorphic questions posed in this study, the geomorphic classification was statistically evaluated with respect to each of the three hydrologic metrics using the same statistical tests. The dominance of hydrologic setting on channel type occurrence (i.e. question 1) was assessed using nonparametric statistical bootstrapping to understand how channel types are distributed across settings relative to equal-probability random occurrence. The dominance of hydrologic setting on reach-scale channel attributes (i.e. question 2) was assessed using a nonparametric Kruskal-Wallis test for each channel attribute in each channel type to test for differences between hydrologic settings. All statistical tests are summarized in Table 2.

Table 2. Statistical tests used to determine if hydrologic setting is a dominant control on reach-scale morphology.

Statistical Tests	Type of statistical test	Significance meaning (<5% probability of occurrence)	Test Abbreviation
<i>Reach-scale channel type tests</i>			
Number of sites in a hydrologic setting (Figure 1, Test a)	Bootstrapping of terciles	The channel type occurs at a higher proportion in a single hydrological setting than randomly expected	B1
Number of hydrologic settings in a channel type (Figure 1, Test a)	Bootstrapping of deciles	The channel type occurs in a lower number of hydrological settings than randomly expected	B2
<i>Reach-scale geomorphic attribute test</i>			
Within channel type differences in attributes (Figure 1, Test b)	Kruskal-Wallis	A given attribute of the channel type displays significant differences between hydrological settings	KW1

Statistical bootstrapping indicates whether a channel type is more or less likely to occur within a given hydrologic setting relative to equal-probability random occurrence. Bootstrapping was conducted by randomly assigning a hydrologic setting to each of the outlier-filtered sites within each channel type. This was repeated 1,000 times to obtain robust statistical expectations of the uniqueness between hydrologic setting and channel type. Two different tests were considered.

First, for each channel type, the percent of sites occurring in each hydrologic metric category was compared between real and bootstrapped datasets (Table 2; B1). If the number of sites in a category (observed results) is indistinguishable from random (bootstrapped results), there is no indication of dominant control on channel type. For a hydrologic setting to dominantly control channel type, we propose that > 70% of hydrologic metric categories across all channel types would deviate from a random number of sites ( $p < 0.05$ ).

The second test compared the number of hydrologic metric categories occurring in a channel type with bootstrapped results (Table 2; B2). Results are deemed significant if the occurrence probability of the observed number of hydrologic metric categories in a channel type is less than 5% when compared to bootstrapping results. For hydrologic setting to dominantly control channel type, we propose that >70% of channel types should deviate from the random number of hydrologic metric categories occurring within a channel type.

Kruskal-Wallis tests were conducted to investigate hydrologic influence on reach-scale channel attributes (Table 2; KW1). The tests were conducted within each channel type between every possible hydrologic setting for two sets of variables: gross dimensional attributes and feature attributes. Slope, bankfull depth, bankfull width, and width-to-depth ratio constitute gross dimensional attributes, which the literature expects to have tight linkages with hydrologic setting. Coefficient of variation in bankfull depth, coefficient of variation in bankfull width, sinuosity,  $D_{50}$ , and  $D_{84}$  are termed feature attributes because the literature has either not significantly investigated their reach-scale linkages with hydrology or they are considered as secondary adjustable fluvial variables. The 'kruskal.test' function (stats package) was used to calculate significance levels. For channel types that only occurred in one hydrologic setting, this analysis was not possible. Therefore, the analysis generated 81 tests for each of the hydrologic metrics (i.e. nine reach-scale attributes tested in nine channel types). To more simply represent all Kruskal-Wallis tests, the results are

presented as a binary plot of statistical significance for each channel attribute in each channel type as seen in the conceptual example of Figure 4. The occurrence of multiple significant returns for a given channel attribute across channel types would indicate that hydrologic setting consistently leads to differences in that channel attribute. We propose that an attribute should show significant differences in >70% of channel types at the 95% confidence level for hydrologic setting to be deemed a dominant control on that attribute. Further investigation into the meaning of significant returns was conducted for channel attributes that showed significance across multiple channel types.

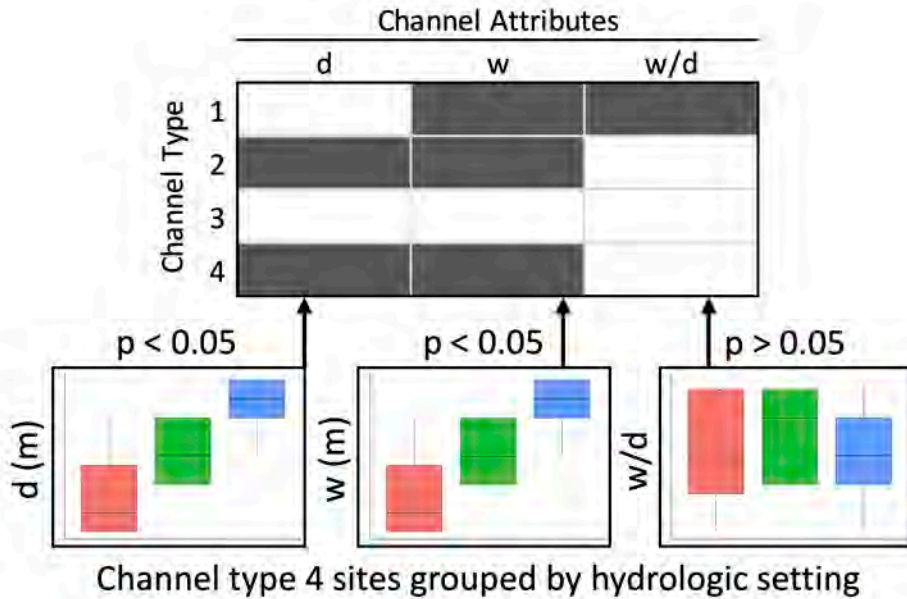


Figure 4. A conceptual example of how individual Kruskal-Wallis tests between hydrologic settings are represented in a compact binary plot for each attribute in each channel type. Box-and-whisker plots are shown for channel type 4 only. A grey box in the binary plot represents a significant difference between hydrologic settings for a given attribute ( $p < 0.05$ ), while a white box represents an absence of a significant difference.

## Results

In the following section we discuss the following key results: (1) the Sacramento River basin exhibits ten distinct channel types, (2) flood magnitude can explain aspects of channel geometry, but not channel type, (3) dimensionless flood magnitude explains the influence of transport capacity in uniform streams, and (4) reach-scale morphology is independent from annual hydrologic regime.

### Ten channel types described by reach-scale morphological classification

Ten channel types, made up of between 4 and 45 sites (site data is summarized and compiled by site in Supplementary Information Tables S1 & S5), were identified using WHC with heuristic refinement and tested for geomorphic significance and performance with a classification tree analysis

(Figs. 5a, 5b, and 6). The compilation of ‘NbClust’ metrics suggests three Ward’s clusters as the optimal number of groupings driven by strong breaks in sediment size and valley confinement. As three groups was insufficient to describe the variability of reach-scale morphology within the basin, secondary indications by Hubert and Arabie values at 10 and 13 groups were the focus of heuristic refinement. The final ten channel types were the result of a heuristic dissolution and aggregation of the WHC dendrogram including the combination of splits in clusters 3 and 7, which outperformed combination with channel types 1 and 10, respectively, under classification tree cross-validation. Physical similarity between combined clusters was confirmed based on analysis of site photography. The classification tree produced a ten-fold cross-validated classification rate of 75%. Further statistical analysis addressing the “Accuracy of reach-scale channel types” can be found in the Supplementary Information. A thorough discussion of the classification in comparison to the Lane et al. (2017b) (Supplementary Information Table S4), Montgomery and Buffington (1997), and Rosgen (1994, 1996) classifications can also be found in the Supplementary Information.

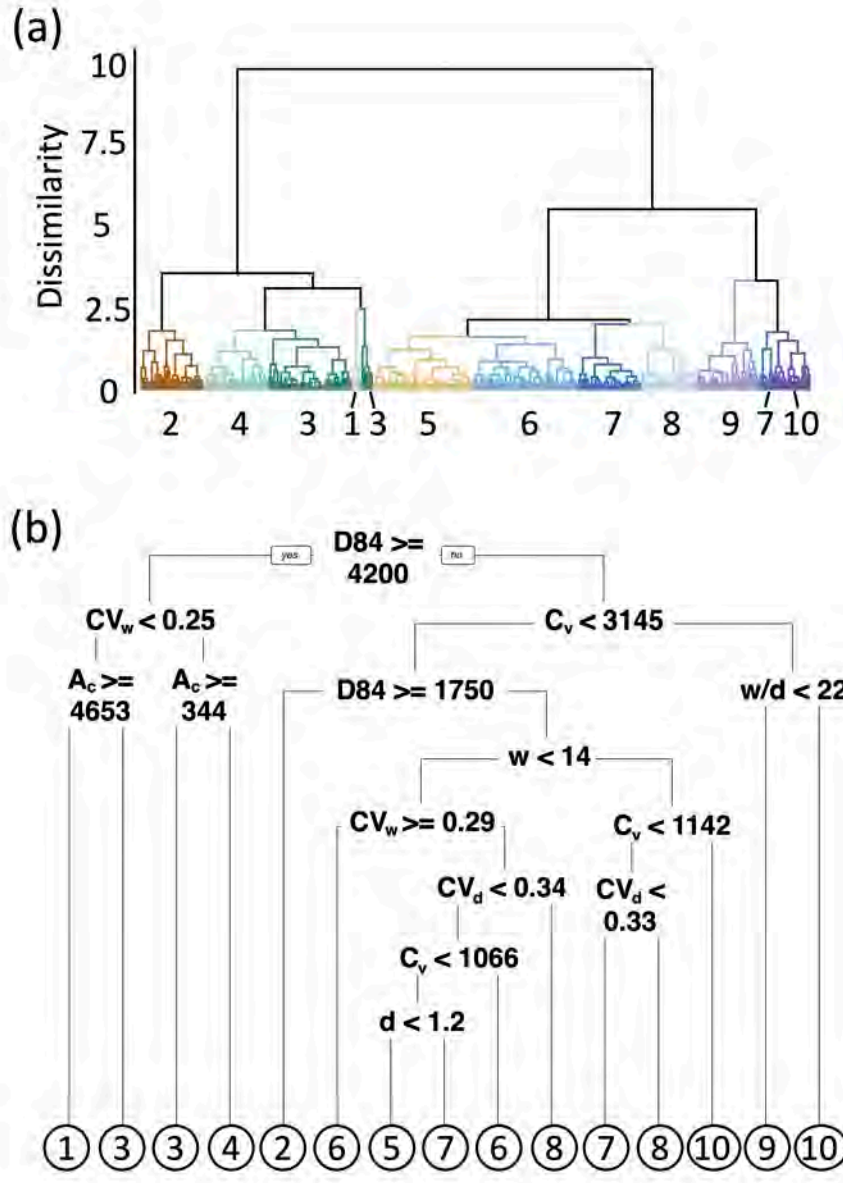


Figure 5. Results from (a) hierarchical clustering by Ward's algorithm analyses, and (b) classification tree analysis. ( $A_c$  is contributing area,  $s$  is surveyed slope,  $d$  is bankfull depth,  $w$  is bankfull width,  $w/d$  is bankfull width-to-depth ratio,  $CV_d$  is coefficient of variation in bankfull depth,  $CV_w$  is coefficient of variation in bankfull width,  $D_{84}$  is sediment size at the 84th percentile, and  $C_v$  is valley confinement; dashed lines only an aid to indicate which attribute is associated with which vector).

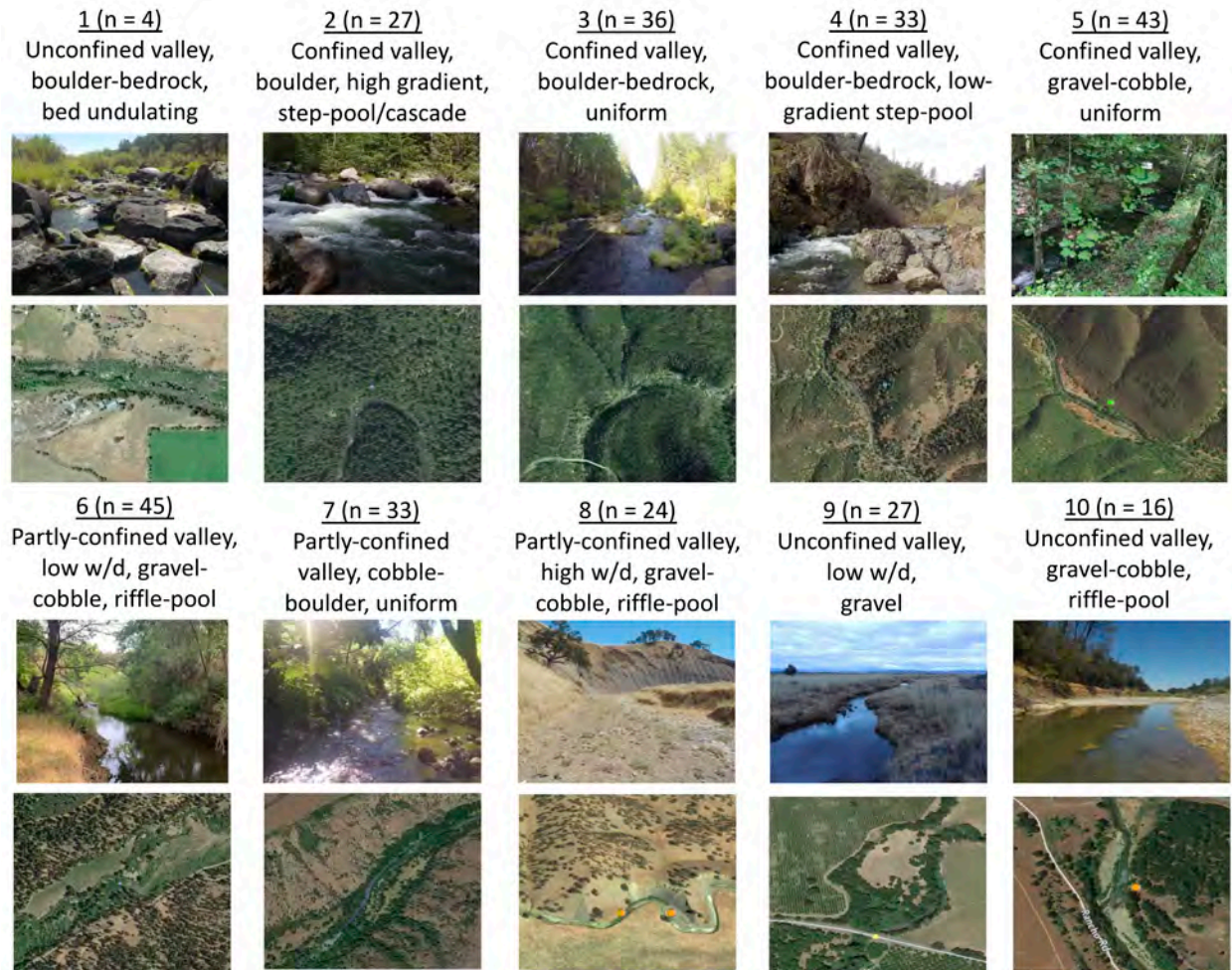


Figure 6. The ten channel types for the Sacramento River basin determined by multivariate statistical analysis with heuristic refinement.

Channel types presented here showed significant differences in every channel attribute used in the geomorphic classification identified by pairwise differences ( $p < 0.05$ ; Fig. 7). Because sediment size and valley confinement play an important role in clustering, the classification is broadly numerically organized from large to small clast size (Fig. 7). Channel types were also generally organized by confinement based on the median valley confinement value of each channel type (Fig. 7). While there was not a high log-log inverse correlation between sediment size and confinement using individual site data ( $R^2 = 0.27$ ,  $p < 0.01$ ; Supplementary Information Fig. S1), there is an inverse relationship between sediment size and valley confinement for median values of channel types 2 through 10 ( $R^2 = 0.65$ ,  $p < 0.01$ ; median channel type attributes are summarized in Supplementary Information Table S2). Figures depicting these relationships can be found in the Supplementary Information. The unconfined valley, boulder-bedrock, bed undulating channel type (channel type 1) exists as a more unique setting within the basin and is discussed below.

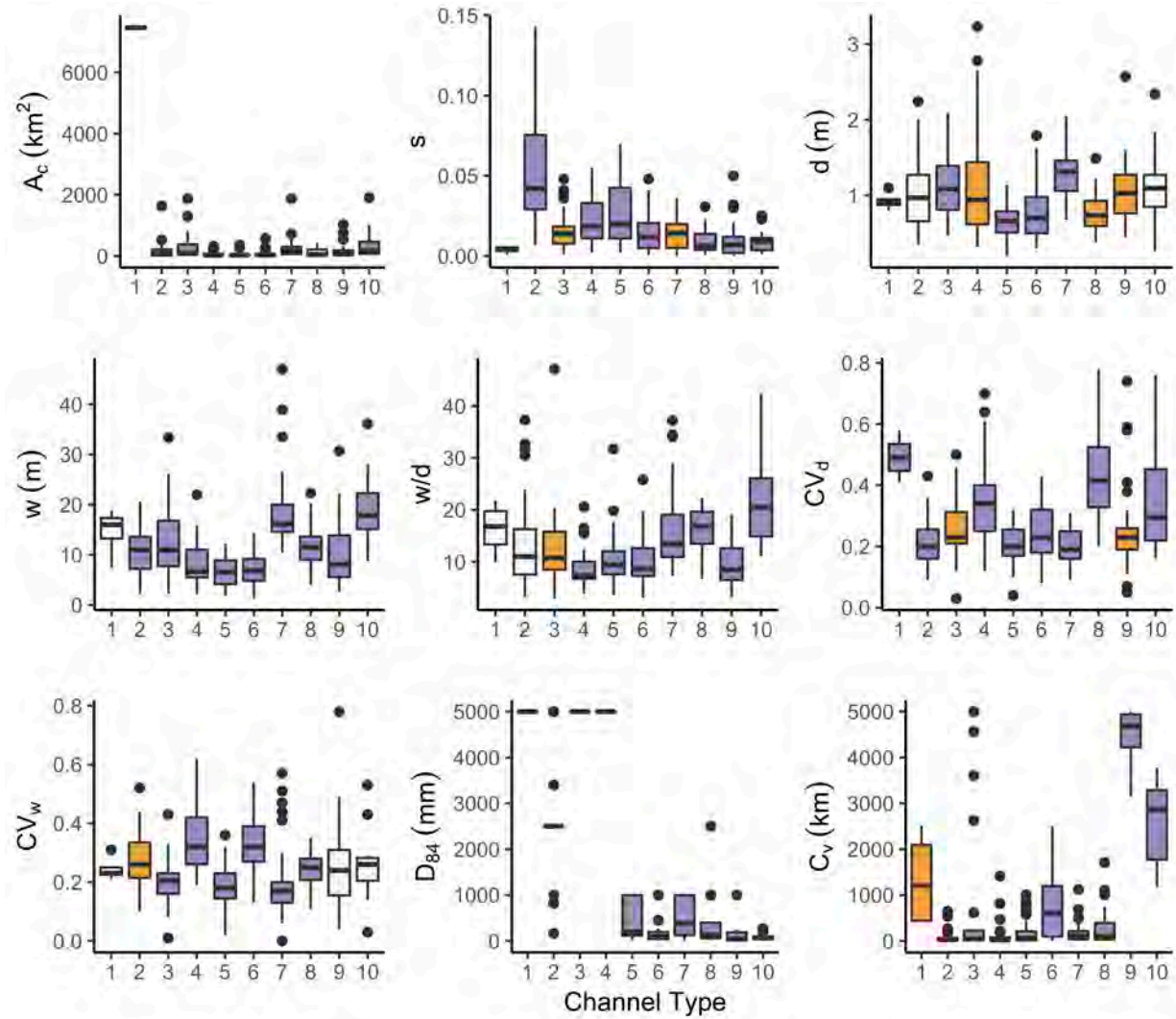


Figure 7. Box and whisker plots representing differences in geomorphic attributes between channel types. Purple boxes represent channel types significantly different than multiple other channel types, orange boxes represent channel types significantly different than one other channel type, and white boxes represent no significant differences from all other channel types ( $p < 0.05$ ). ( $A_c$  is contributing area,  $s$  is surveyed slope,  $d$  is bankfull depth,  $w$  is bankfull width,  $w/d$  is bankfull width-to-depth ratio,  $CV_d$  is coefficient of variation in bankfull depth,  $CV_w$  is coefficient of variation in bankfull width,  $D_{84}$  is sediment size at the 84th percentile, and  $C_v$  is valley confinement.)

Given the relationship between confinement and sediment size, the classification generally progresses from confined, mountainous upland streams with large sediment sizes to unconfined, lowland streams and rivers with small sediment. A notable exception is the unconfined valley, boulder-bedrock, bed undulating channel type, which fits within the conceptual framework of large to small sediment size rivers, but the sites exist in predominantly unconfined valleys. This lack of confinement indicates colluvial and mass movement processes are unlikely in these settings. Therefore, the large sediment clasts and unique Modoc Plateau volcanic terrain at these locations are either transported from upstream or non-fluvial legacy deposits of the underlying volcanic terrain (Hauer and Pulg, 2018). The uniqueness of this channel type likely means that hydrologic metrics presented below have less

influence.

## **Flood magnitude can explain aspects of channel geometry, but not channel type**

Statistical bootstrapping of flood magnitude settings showed the most significant returns, but below the 70% threshold (Fig. 8a & 8b). It should be noted that unlike the conceptual examples of bar plots given in graphics a1 and a2 of Figure 1, columns are not of the same height in Figure 8 due to unequal sampling of the channel types. However, the same tests can be applied. For test B1, 18.5% of tercile flood magnitude settings were significant (splits for low, medium, and high flood magnitude defined at 64 and 194 m<sup>3</sup>/s) ( $p < 0.05$ ; Fig. 8a). For test B2, which used decile flood magnitude settings (splits defined at 20.9, 34.9, 56.2, 92.8, 122.7, 152.1, 238.6, 373.9, and 592.7 m<sup>3</sup>/s), the number of hydrologic settings was significant for 40% of channel types ( $p < 0.05$ ; Fig. 8b). Both results indicate that certain channel types exhibit basin scale flood magnitude-morphology relationships, but similarities in reach-scale morphology appear predominantly governed by other factors. Therefore, flood magnitude does not appear to be a dominant control on form between channel types but is rather only correlated to certain forms based on where a specific channel type is found in the drainage network.

While flood magnitude does not capture differences between channel types, it does explain differences in channel geometry within multiple channel types (test KW1). Significant differences in gross geometry attributes exist across channel types (Fig. 8c). Bankfull width shows significant differences between flood magnitude settings in 67% of channel types ( $p < 0.05$ ), which nearly exceeds the proposed significant threshold. Because flood magnitude was calculated from contributing area - discharge regressions, the significant differences associated with bankfull width are linked to well-established downstream hydraulic geometry relationships. Positive relationships between bankfull width and flood magnitude exist for several step-pool, uniform, and riffle-pool channel types as well as the channel type that qualitatively includes anastomosed channels (channel type 9). When combined, all basin sites demonstrate a clear relationship between bankfull width and flood magnitude ( $R^2 = 0.56$ ,  $p < 0.01$ ), and these relationships hold true within individual channel types as well.



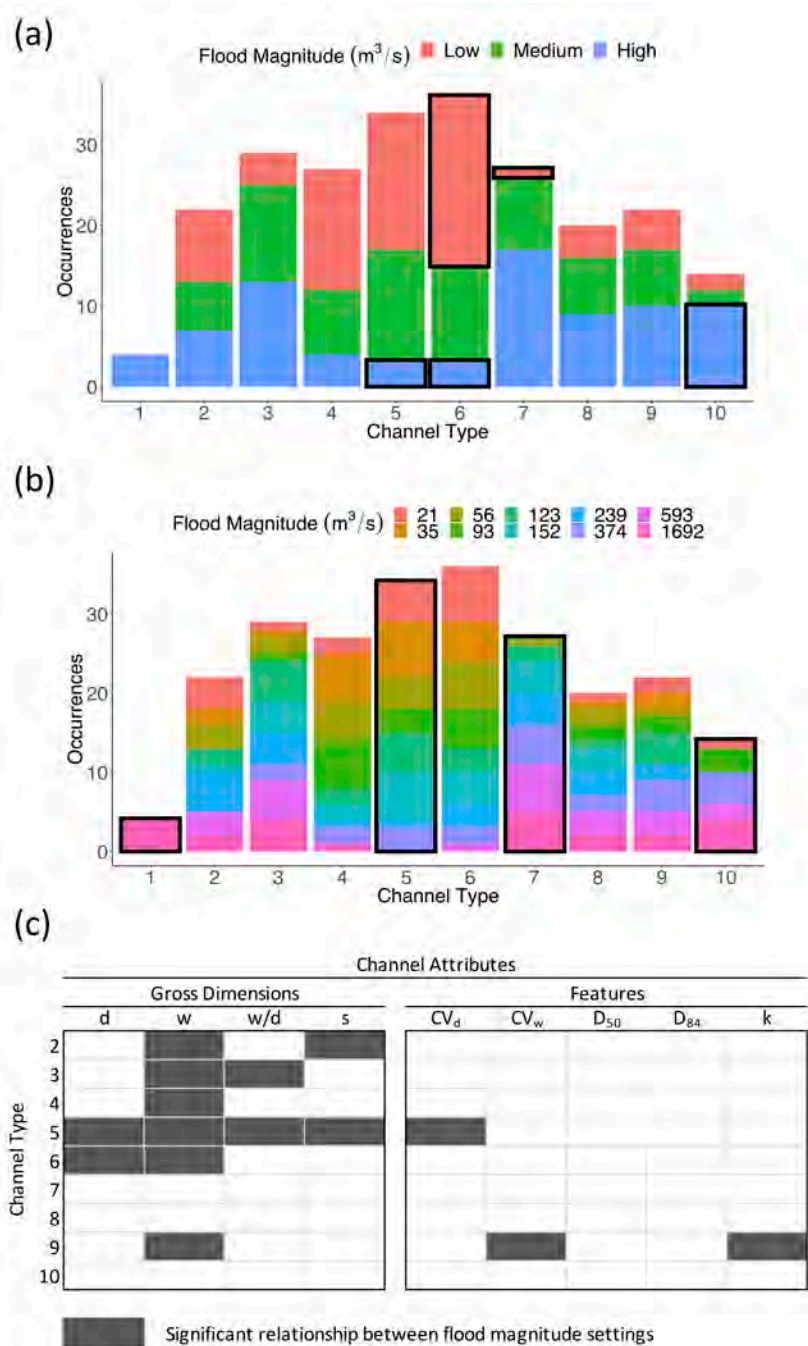


Figure 8. Statistical analysis of reach-scale morphology – flood magnitude relationships including (a) the proportion of each channel type falling within tercile bins (statistical test B1), (b) the proportion of each channel type falling within ten quantile bins labeled by the upper value of flood magnitude (statistical test B2), and (c) a binary display of channel attribute significance between flood magnitude categories within a channel type (statistical test KW1). In the bar plots, black borders indicate that (a) the number of channel type sites within a hydrologic setting or (b) the number of hydrologic settings within a channel type have a less than 5% probability of occurrence when compared to bootstrapping results. In (c), a grey rectangle represents a significant difference ( $p < 0.05$ ).

## Dimensionless flood magnitude best represents transport capacity, but not channel type occurrence

Statistical bootstrapping results suggest that dimensionless flood magnitude does not control channel type presence (Fig. 9a & 9b). Under test B1, the number of hydrologic setting occurrences was significant in 17% of bins (low, medium, and high dimensionless flood magnitude split at 0.83 and 2.41) ( $p < 0.05$ ; Fig. 9a). For test B2, 30% of channel types displayed a significant number of 10-bin hydrologic settings (splits defined at dimensionless flood magnitudes of 0.27, 0.48, 0.76, 1.06, 1.40, 1.83, 2.61, 4.56, and 9.40) ( $p < 0.05$ ; Fig. 9b). Both results are well below the suggested 70% threshold and are likely the result of spurious correlation between channel attributes and channel type. That is, streams with relatively small and large sediment sizes exhibit high and low dimensionless flood magnitude values, respectively. Therefore, dimensionless flood magnitude appears to be a poor indicator of reach-scale morphology overall.

While the majority of significant values were associated with feature attributes, dimensionless flood magnitude settings showed significant differences in slope, a gross dimensional attribute (test KW1; Fig. 9c). In four channel types including cascade/step-pool (channel type 2), cobble uniform streams (channel types 5 and 7), and high w/d riffle-pool (channel type 8), slope was found to be significantly lower in sites with high dimensionless flood magnitudes. In uniform streams, the lack of variability in channel depth and width and the expression of slope as a critical factor in reach-scale morphology is logical because equivalent transport capacities needed to transport equivalent sediment yields can be achieved with increased slope and decreased flow or decreased slope and increased flow (Lane, 1954). Other factors in greater variability channel types may dampen this slope relationship. The remaining significant attributes are dominated by feature attributes, predominantly  $D_{50}$  and  $D_{84}$ , which are likely attributable to spurious correlation rather than physical significance. Unlike channel width (Leopold and Maddock, 1953), sediment size is generally negatively correlated with contributing area or discharge for 2nd order and larger streams (Brummer and Montgomery, 2003; Knighton, 1980). This results in an inverse relationship between dimensionless flood magnitude, as calculated here, and sediment size, meaning that significant differences are likely to be accentuated in this analysis for  $D_{50}$  and  $D_{84}$ .

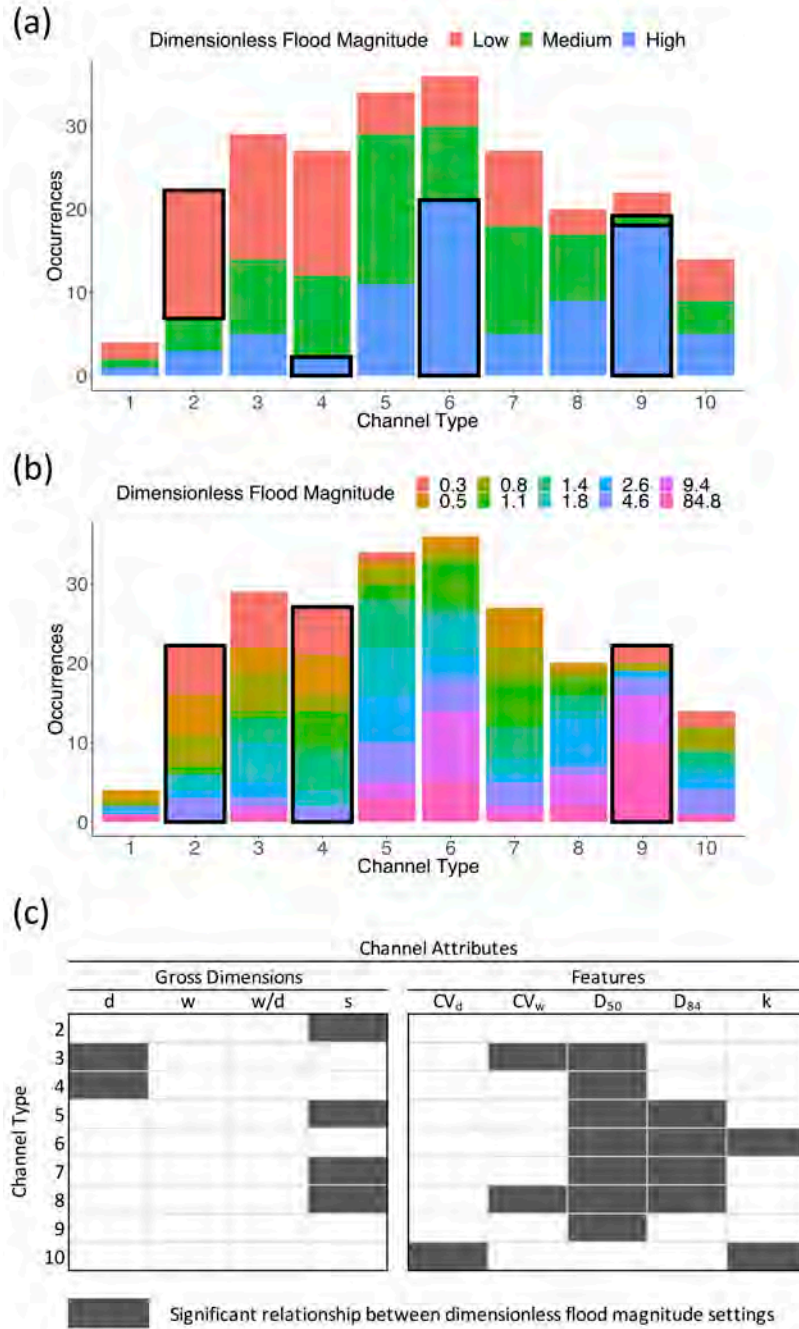


Figure 9. Statistical analysis of reach-scale morphology – dimensionless flood magnitude relationships including (a) the proportion of each channel type falling within tercile bins (statistical test B1), (b) the proportion of each channel type falling within ten quantile bins labeled by the upper value of dimensionless flood magnitude (statistical test B2), and (c) a binary display of channel attribute significance between dimensionless flood magnitude bins within a channel type (statistical test KW1). In the bar plots, black borders indicate that (a) the number of channel type sites within a hydrologic setting or (b) the number of hydrologic settings within a channel type have a less than 5% probability of occurrence when compared to bootstrapping results. In (c), a grey rectangle represents a significant difference ( $p < 0.05$ ).

## Reach-scale morphology is independent of annual hydrologic regime

Statistical bootstrapping revealed that the occurrences of hydrologic settings within a given channel type were rarely significant and thus the hydrogeomorphic linkage was random (Fig. 10a & 10b). For test B1, the number of sites within a hydrologic setting for each channel type was found to be significant in 6% of all bins ( $p < 0.05$ , Fig. 10a). All significant findings are likely explained by the landscape features important in defining the annual hydrologic regime. For example, 67% of low width-to-depth, gravel sites (channel type 9) exist within the Rain and Seasonal Groundwater streams of the Central Valley, which are characterized by relatively low slopes ( $<1\%$ ), agricultural land use, and at times anastomosed streams. Test B2 showed that there was minimal significance when investigating how many hydrologic settings a channel type occurs in with only 20% of channel types showing significance ( $p < 0.05$ ; Fig. 10b). These significant returns are complementary to the test B1 and likely a product of their landscape setting at the sub-basin scale rather than hydrology controlling the channel type. Both statistical tests fell well below the threshold of 70% proposed to indicate clear hydrologic setting control of channel types. Results of 6% and 20% are far below any reasonable definition of dominant physical control of one variable over another.

Hydrologic setting was found to drive differences in gross dimensional channel attributes within a channel type to a greater extent than feature attributes, but still below a level of dominant control (statistical test KW1; Fig. 10c). No attribute was significant across more than 44% of channel types. Significant differences in width are likely indicative of hydraulic geometry differences between annual hydrologic regimes. For example, bankfull width was significantly higher in RGW settings ( $p < 0.05$ ), which generally coincide with higher order streams lower in the basin. However, significance in  $w/d$  does not show the same consistency as  $w$  since it both increases and decreases in tandem with hydrologic setting in some cases ( $p < 0.05$ ). This precludes a simple explanation of the patterning of significance for  $w/d$  and may be due to landscape setting. Significant returns associated with slope may also be a result of landscape setting. Landscape influence can be observed as streams in three of nine channel types are significantly steeper in Low Volume Snowmelt and Rain stream sites ( $p < 0.05$ ), which also relates to the mountainous terrain in which this hydrologic setting is found.

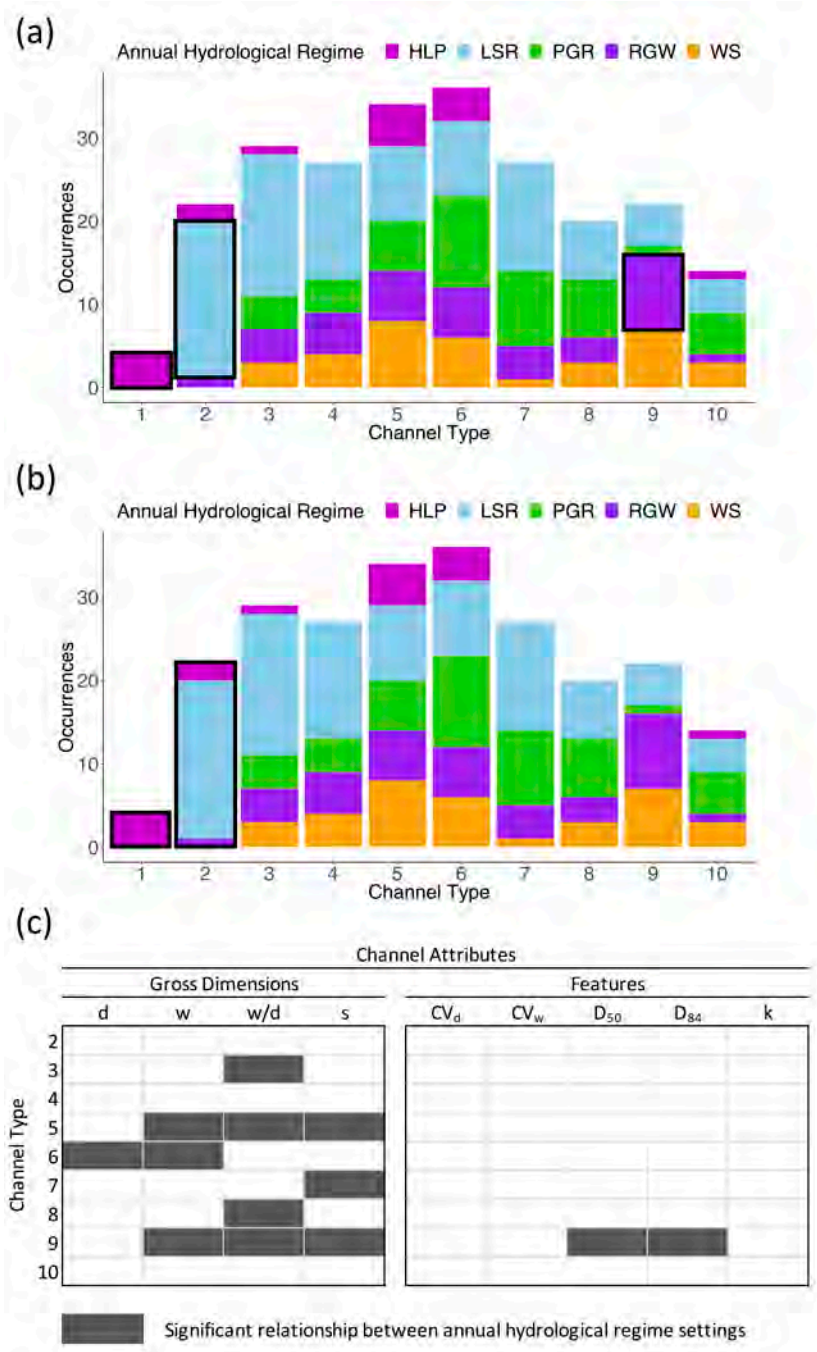


Figure 10. Statistical analysis of reach-scale morphology – annual hydrologic regime relationships including (a) the proportion of each channel type falling within tercile bins (statistical test B1), (b) the proportion of each channel type falling within each annual hydrologic regime bin (statistical test B2), and (c) a binary display of channel attribute significance between annual hydrologic regime bins within a channel type (statistical test KW1). In the bar plots, black borders indicate that (a) the number of channel type sites within a hydrologic setting or (b) the number of hydrologic settings within a channel type have a less than 5% probability of occurrence when compared to bootstrapping results. In (c), a grey rectangle represents a significant difference ( $p < 0.05$ ).

## Discussion

### Channel types exist across all hydrologic settings

Contrary to the hypothesis that certain channel types only occur in certain hydrologic settings, study results demonstrate that channel types almost always exist across all hydrologic settings. The few channel types preferentially occurring in certain hydrologic settings can be attributed to relationships between median geomorphic attributes and hydrologic settings (e.g. hydraulic geometry). However, even for significant hydrogeomorphic relationships, hydrologic setting does not preclude those channel types from also existing in other settings. Therefore, hydrologic setting is unlikely to be the dominant control on channel morphology or, if initially the dominant control, it is consistently dampened throughout the channel network by other local processes that create each of various channel types. This indicates that reach-scale morphology must be a product of other geomorphic influences such as sediment regime, topography, geology, or a specific interaction of hydrology with these influences.

Channel hydraulics, a product of hydrology and topographic steering, play an important role in the formation of morphological units. Differences in hydraulics have been hypothesized as controls in the formation of various channel types, such as riffle-pool and step-pool channels (Church and Zimmermann, 2007; MacWilliams et al., 2006; Thompson, 1986; Zimmermann et al., 2010). In the case of channel hydraulics, hydrologic setting is more likely to change acutely at stream confluences, while topography can show abrupt, complex longitudinal change between tributary junctions, especially in mountainous terrain (Wohl, 2000). Variability among topographic attributes can be independent or linked, yielding different functional landforms, and then these may be hierarchically nested at different flow stages to further complicate hydraulics and drive different morphological outcomes (Pasternack et al., 2018a, 2018b). This supports the idea that the existence of a given channel type is perhaps less informed by hydrologic setting and instead driven by topographic influences.

Sediment supply or non-fluvial bed material may also impact reach-scale morphology more directly than hydrologic setting (Church, 2006; Friend, 1993; Harvey, 1991; Hauer and Pulg, 2018). Although substantial geomorphic change is often related to flood events, the sediment characteristics may control specific changes to channel form more than the amount of water (Wohl et al., 2015). For example, Tooth and Nanson (2004) demonstrate two arid region rivers with similar discharge regimes but different morphologies partially attributed to sediment caliber. In conjunction and at a continental scale, Phillips and Jerolmack (2016) concluded that channels self-organize shape to achieve a critical shear depth needed to transport available bed sediments during floods, which is exemplified by studies of bar and channel pattern dynamics associated with sediment fluxes in dammed and dam removal settings (East et al., 2015, 2018; Melis et al., 2012). Both examples point to reach-scale sediment conditions as important drivers of channel morphology.

In regard to the channel classification presented here, confined low-order streams are likely subjected to episodic but infrequent lateral inputs of sediment by mass movement events, while unconfined low gradient and high-order streams are likely subjected to more gradual, longitudinal sediment inputs (Benda and Dunne, 1997b, 1997a; Benda et al., 2004; Grant and Swanson, 1995). Sloan et al. (2001) noted that valley floor modification is less dependent on the magnitude and frequency of in-channel flood events and more dependent on the denudation of landscapes and mass movement events. Because results presented here show that the hydrologic metrics are not statistically related to the occurrence of channel types, it is possible that sediment supply in combination with sediment

size would be a better indicator of reach-scale morphology. Further, the known land-use changes across the Sacramento River basin and alterations in sediment regimes in a number of rivers may further drive dependence of channel types on sediment supply (Gilbert, 1917; James, 1991; White et al., 2010). Site specific sediment regimes were not the focus of this study but are an important avenue for future research.

Qualitative reasoning provides a partial understanding of the disconnection between hydrologic setting and reach-scale morphology. For a specified stream location, observations of the reach-scale hydrology responsible for a given form are difficult to obtain except following a large channel-altering flood event (Dean and Schmidt, 2013). It may be possible to estimate bankfull channel discharge or flow depth necessary to entrain bed sediments, but when a flow has occurred and to what extent the channel shape was altered are complex questions. Further complicating the relationships between form and hydrology, different channel types are likely formed and maintained under different flow magnitudes (Knighton, 1998). Similar forms are also found within different climatic conditions (e.g. temperate vs. arid) and thus subjected to large differences in annual hydrologic conditions (Wohl and Merritt, 2008). In comparison, biological characteristics along a river reach are likely to display indicators related to recent flow patterns or events (e.g. riparian recruitment) and flows over longer periods of time (e.g. plant senescence) (Polvi et al., 2011). The fact that geomorphic characteristics are likely less relatable to recent flow events than through biological indicators may simply be representative of the low and high influences hydrologic setting has on reach-scale channel types and biological conditions, respectively. Individual morphological units can also be formed by local processes, for example in the formation of forced pool or riffle conditions involving bedrock or large woody debris (Fryirs and Brierley, 2012; Montgomery and Buffington, 1998). This clear evidence of morphological unit formation points toward local valley influences being key drivers of reach-scale morphology as opposed to hydrologic setting as local geomorphic influences can dictate thresholds of geomorphic form (Montgomery, 1999; Poff et al., 2006).

## **Hydrologic setting does not control topographic variability of channel dimensions**

A number of extremal hypotheses have been suggested for the development of repeating channel patterns and forms, and the majority fit within the context of the minimum energy principle (Huang et al., 2004). With depth variability shown here to be unrelated to hydrologic settings and bedforms being a major component of energy dissipation in rivers (Davies and Sutherland, 1980), it would suggest that the nature of energy dissipation induced by stream form is primarily controlled by factors other than hydrologic setting (e.g. lithology, topography, sediment supply). Langbein and Leopold (1964) note two distinct sources of variance in channels: that associated with variation around an average condition as a system searches for equilibrium and that which exists in any natural system because of local factors that make two systems inherently different. The latter form of variance at a sub-basin scale could conceptually be represented by distinct channel types. This would mean that channel types are far more dependent on local valley topography and sediment supply. Extreme hydrologic events that have been observed to cause large changes in channel width and pattern (Yochum et al., 2017) may be representative of variance around the average condition. This result would suggest that channels take the reach-scale morphology of local conditions and that reach-scale morphology is dimensionally adjusted to the continuum basin conditions such as those defined by downstream hydraulic geometry relationships.

Results from all hydrogeomorphic analyses show relatively few significant differences in TVA values by hydrologic setting. TVAs were identified as key attributes in distinguishing channel types, and

different channel types exhibit differences in hydraulic patterns relevant to ecological functioning (Lane et al., 2018a). The hydrologic metrics evaluated here do not capture significant differences in TVAs, and consequently do not control variability in channel dimensions. Montgomery (1999) conceptualized that continuum processes would likely be more influential on channel size, while channel morphology would be dependent on local controls. This study confirms that concept by showing that TVA values are not influenced by hydrologic setting. This is complementary to the fact that hydraulic geometry relationships exhibit variability around a median condition that cannot be ascribed to sub-basin hydrology (Park, 1977). If variability in form is not controlled by hydrologic setting, then it is logical that reach-scale channel types, which are often defined by characteristic bedforms, are not related to hydrologic settings across a basin. Therefore, future predictions of reach-scale morphology across entire networks should strive to quantify local geologic, topographic, and sediment supply attributes of the landscape. With rapidly expanding high-resolution data sources and computational power, techniques such as machine learning may be effective to achieve more complete understanding of controls on topographic variability and reach-scale channel types (Guillon et al., 2020).

## Hydrologic analysis constraints

Although reach-scale hydrologic settings provide limited information about the likelihood of occurrence of a given channel type, study results do not preclude hydrologic influence on reach-scale morphology, such as through site-specific hydrology. Historical flow conditions are likely to play a role in channel pattern at a minimum and when thinking about at-a-station form at different flow magnitudes (Heitmuller et al., 2015). Channel-width expansion and contraction cycles have been linked to hydrologic disturbance events (Dean and Schmidt, 2013; Pizzuto, 1994; Sholtes et al., 2018) and long-term effects of natural and anthropogenic alterations to river systems (Friedman et al., 2015; Grams and Schmidt, 2002; Swanson et al., 2011). These documented impacts of hydrologic change occur in channels where width expansion is possible and are likely related to classic relationships of single and multi-threaded channels and discharge (Leopold and Wolman, 1957; Schumm, 1977). Our final reach-scale classification lacks a braided, gravel-bed river type which precludes the comparison between single and multi-threaded river channels in this study. Even with a braided channel type, at-a-station hydrologic records are probably much more important to channel types than more readily available extrapolated or modeled hydrologic information.

Beyond historical flow events, consistent nuanced differences in at-a-station hydrology may also play a role in reach-scale morphology. Given that channel hydraulics create and maintain various morphological units and that hydraulics are a product of hydrology as well as topographic steering and biological influences, there may be differences in sub-basin hydrology at reach-scales associated with changing landscape conditions. Deal et al. (2018) note that climatic signals are often muted across basins due to landscape characteristics. Locations with less muted climatic signals and exhibiting median basin-scale hydrology may also display median hydraulic geometry tendencies. However, locations that do not display expected hydrology may lead to the scatter of channel types across hydrologic settings observed here. For example, in conjunction with distinct changes in slope and confinement, basin hydrology is observed to be highly altered on alluvial fans or in alpine meadows (Hooke, 1967; McClymont et al., 2010). A second possibility is that hydrologic influences are most impactful at small catchment scales (Gomi et al., 2002). It is possible for two headwater basins to have distinctly different retention capacity and therefore different flood characteristics. Differences in hydrologic inputs from these two basins would impact reach-scale morphology. For



example, if a headwater basin is prone to debris flow conditions and is directly connected to a confined stream (Brummer and Montgomery, 2003; Rathburn et al., 2018), that basin will contribute considerably more sediment to the stream compared to a disconnected or low-sediment basin. If differences in debris flow susceptibility are driven by differences in hydrology, then hydrology is the key driver in that system. Recovery times of channels subjected to disturbances would also be dependent on hydrology (Wohl and Pearthree, 1991). Finally, reach-scale hydrologic dynamics may also play a role in the vegetation assemblage, which can influence local morphology through processes such as bank or bar stabilization and channel narrowing (Gurnell, 2014). Therefore, hydrologic importance does not necessarily need to be linked to the hydrologic settings that were examined here.

While results showed that hydrologic setting is a poor indicator of channel type, results may differ in basins with more unique hydrologic settings. We may expect to find a number of cases where the findings presented here do not hold true, especially in peculiar places (Grant and O'Connor, 2003). While all rivers are unique, certain hydrologic settings show more distinct characteristics. For example, rivers in karst environments have complex hydrodynamic and erosional characteristics that ultimately lead to substantial differences in hydrology and morphological form (Ford and Williams, 2007; Ritter et al., 1995). At these locations hydrogeomorphic correlations may be considerably more distinct. Other peculiar river environments likely exist that are observable as hydrologic settings, which would also contradict our findings. Further research on the uniqueness of hydrologic settings across larger areas may prove to be important to decipher areas where hydrologic settings may play a role in channel form beyond hydraulic geometry relationships.

Given that the Sacramento River basin has been subjected to numerous hydrogeomorphic alterations, the basin itself could be one of the aforementioned peculiar places. It may be that the results presented here are not the norm and similar methodologies used in other portions of the world would show strong dependence of reach-scale channel types on hydrologic setting. However, this is unlikely for two reasons. First, almost all rivers around the world have faced some anthropogenic impacts, so the idea of finding perfect locations to test the premise of this study is questionable. Second, in defense of the relevance of the Sacramento River basin for such testing, the results presented here conform with long standing hydrogeomorphic concepts of a link between form and process, such as predictable downstream hydraulic geometry. Hydrologic setting does display a noticeable relationship with bankfull width. This discharge-based control on channel size contradicts the view that the basin is too heavily impacted to show real hydrologic controls. In consequence, the fact that reach-scale channel types do not appear to align with hydrologic settings in this study indicates that similar findings are likely in other locations.

## Conclusions

This study sought to address whether hydrologic settings are indicative of reach-scale morphology or, alternatively, whether reach-scale morphology exists independently of hydrologic settings within a basin. Statistically-derived channel types in the Sacramento River basin, a moderately sized catchment with high topographic and hydrologic variability, were found to exist across almost all hydrologic settings examined. Statistical bootstrapping results indicate that continuum hydrology is not a dominant control on classified reach-scale morphologies, but does influence channel dimensions. Results further suggest that even median channel dimensions are often influenced by other geomorphic processes or controls. Given the hierarchical nature of rivers, this analysis only focuses on one

scale of basin and channel morphology so hydrology may still be an observable control at other scales. Isolation of potential controls, such as hydrology, sediment supply, topography, and local geomorphic drivers, can infer the level of influence each has on reach-scale morphology through the rigorous statistical methodologies presented here and should be pursued in future studies to further inform classification-based river management strategies.

## References

- Bard A, Renard B, Lang M, Giuntoli I, Korck J, Koboltschnig G, Janža M, d'Amico M, Volken D. 2015. Trends in the hydrologic regime of Alpine rivers. *Journal of Hydrology* 529: 1823–1837. DOI: 10.1016/j.jhydrol.2015.07.052
- Beechie T, Buhle E, Ruckelshaus M, Fullerton A, Holsinger L. 2006. Hydrologic regime and the conservation of salmon life history diversity. *Biological Conservation* 130: 560–572. DOI: 10.1016/j.biocon.2006.01.019
- Beechie T, Imaki H. 2014. Predicting natural channel patterns based on landscape and geomorphic controls in the Columbia River basin, USA. *Water Resources Research* 50: 39–57. DOI: 10.1002/2013WR013629
- Benda L, Dunne T. 1997a. Stochastic forcing of sediment routing and storage in channel networks. *Water Resources Research* 33: 2865–2880. DOI: 10.1029/97WR02387
- Benda L, Dunne T. 1997b. Stochastic forcing of sediment supply to channel networks from landsliding and debris flow. *Water Resources Research* 33: 2849–2863. DOI: 10.1029/97WR02388
- Benda LEE, Poff NL, Miller D, Dunne T, Reeves G, Pess G, Pollock M. 2004. The network dynamics hypothesis: how channel networks structure riverine habitats. *BioScience* 54: 413–427.
- Bisson PA, Montgomery DR, Buffington JM. 1996. Valley segments, stream reaches, and channel units. *Methods in stream ecology* : 23–52.
- Brierley GJ, Fryirs K. 2000. River Styles, a Geomorphic Approach to Catchment Characterization: Implications for River Rehabilitation in Bega Catchment, New South Wales, Australia. *Environmental Management* 25: 661–679. DOI: 10.1007/s002670010052
- Brummer CJ, Montgomery DR. 2003. Downstream coarsening in headwater channels. *Water Resources Research* 39: 1294, 1-14. DOI: 10.1029/2003WR001981 [online] Available from: <https://agupubs.onlinelibrary.wiley.com/doi/abs/10.1029/2003WR001981> (Accessed 11 September 2018)
- Buffington JM, Lisle TE, Woodsmith RD, Hilton S. 2002. Controls on the size and occurrence of pools in coarse-grained forest rivers. *River Research and Applications* 18: 507–531. DOI: 10.1002/rra.693
- Carson MA. 1972. Hillslope form and process . University Press: Cambridge
- Carson MA. 1984. The meandering-braided river threshold: A reappraisal. *Journal of Hydrology* 73: 315–334. DOI: 10.1016/0022-1694(84)90006-4
- Chang HH. 1979. Minimum stream power and river channel patterns. *Journal of Hydrology* 41: 303–327. DOI: 10.1016/0022-1694(79)90068-4

- Chin A, Wohl EE. 2005. Toward a theory for step pools in stream channels. *Progress in Physical Geography: Earth and Environment* 29: 275–296. DOI: 10.1191/0309133305pp449ra
- Church M. 2002. Geomorphic thresholds in riverine landscapes. *Freshwater biology* 47: 541–557.
- Church M. 2006. Bed Material Transport and the Morphology of Alluvial River Channels. *Annual Review of Earth and Planetary Sciences* 34: 325–354. DOI: 10.1146/annurev.earth.33.092203.122721
- Church M, Zimmermann A. 2007. Form and stability of step-pool channels: Research progress. *Water Resources Research* 43: W03415, 1-21. DOI: 10.1029/2006WR005037 [online] Available from: <https://agupubs.onlinelibrary.wiley.com/doi/abs/10.1029/2006WR005037> (Accessed 27 August 2018)
- Dahm CN, Grimm NB, Marmonier P, Valett HM, Vervier P. 1998. Nutrient dynamics at the interface between surface waters and groundwaters. *Freshwater Biology* 40: 427–451. DOI: 10.1046/j.1365-2427.1998.00367.x
- Davies TR, Sutherland AJ. 1980. Resistance to flow past deformable boundaries. *Earth Surface Processes* 5: 175–179.
- Davies TRH, Sutherland AJ. 1983. Extremal hypotheses for river behavior. *Water Resources Research* 19: 141–148. DOI: 10.1029/WR019i001p00141
- Deal E, Braun J, Botter G. 2018. Understanding the Role of Rainfall and Hydrology in Determining Fluvial Erosion Efficiency. *Journal of Geophysical Research: Earth Surface* 123: 744–778. DOI: 10.1002/2017JF004393
- Dean DJ, Schmidt JC. 2013. The geomorphic effectiveness of a large flood on the Rio Grande in the Big Bend region: Insights on geomorphic controls and post-flood geomorphic response. *Geomorphology* 201: 183–198. DOI: 10.1016/j.geomorph.2013.06.020
- De'ath G, Fabricius KE. 2000. Classification and Regression Trees: A Powerful yet Simple Technique for Ecological Data Analysis. *Ecology* 81: 3178–3192. DOI: 10.1890/0012-9658(2000)081[3178:CARTAP]2.0.CO;2
- Dettinger M. 2016. Historical and Future Relations Between Large Storms and Droughts in California. *San Francisco Estuary and Watershed Science* 14: 1-21. DOI: <https://doi.org/10.15447/sfews.2016v14iss2art1> [online] Available from: <https://escholarship.org/uc/item/1hq3504j> (Accessed 27 February 2020)
- East AE, Pess GR, Bountry JA, Magirl CS, Ritchie AC, Logan JB, Randle TJ, Mastin MC, Minear JT, Duda J J, Liermann MC, McHenry ML, Beechie TJ, Shafroth PB. 2015. Large-scale dam removal on the Elwha River, Washington, USA: River channel and floodplain geomorphic change. *Geomorphology* 228: 765–786. DOI: 10.1016/j.geomorph.2014.08.028
- East AE, Logan JB, Mastin MC, Ritchie AC, Bountry JA, Magirl CS, Sankey JB. 2018. Geomorphic Evolution of a Gravel-Bed River Under Sediment-Starved Versus Sediment-Rich Conditions: River Response to the World's Largest Dam Removal. *Journal of Geophysical Research: Earth Surface* 123: 3338–3369. DOI: 10.1029/2018JF004703
- ESRI. 2016. ArcGIS Desktop . Environmental Systems Research Institute: Redlands, CA
- Filzmoser P, Garrett RG, Reimann C. 2005. Multivariate outlier detection in exploration geochemistry. *Computers & Geosciences* 31: 579–587. DOI: 10.1016/j.cageo.2004.11.013

- Filzmoser P, Gschwandtner M. 2012. mvoutlier: Multivariate outlier detection based on robust methods. R package version 2.0.9. <https://CRAN.R-project.org/package=mvoutlier>
- Flores AN, Bledsoe BP, Cuhaciyar CO, Wohl EE. 2006. Channel-reach morphology dependence on energy, scale, and hydroclimatic processes with implications for prediction using geospatial data. *Water Resources Research* 42: W06412, 1-15. DOI: 10.1029/2005WR004226 [online] Available from: <https://agupubs.onlinelibrary.wiley.com/doi/abs/10.1029/2005WR004226> (Accessed 12 September 2018)
- Ford D, Williams PW. 2007. *Karst hydrogeology and geomorphology* . [Rev. ed.]. John Wiley & Sons: Chichester, England ; Hoboken, NJ
- Friedman JM, Vincent KR, Griffin ER, Scott ML, Shafroth PB, Auble GT. 2015. Processes of arroyo filling in northern New Mexico, USA. *Geological Society of America Bulletin* 127: 621–640.
- Friend PF. 1993. Control of river morphology by the grain-size of sediment supplied. *Sedimentary Geology* 85: 171–177. DOI: 10.1016/0037-0738(93)90081-F
- Frissell CA, Liss WJ, Warren CE, Hurley MD. 1986. A hierarchical framework for stream habitat classification: Viewing streams in a watershed context. *Environmental Management* 10: 199–214. DOI: 10.1007/BF01867358
- Fryirs KA, Brierley GJ. 2012. *Geomorphic Analysis of River Systems: An Approach to Reading the Landscape* . John Wiley & Sons, Ltd: Chichester, UK [online] Available from: <http://doi.wiley.com/10.1002/9781118305454> (Accessed 31 July 2018)
- Fryirs KA, Wheaton JM, Brierley GJ. 2016. An approach for measuring confinement and assessing the influence of valley setting on river forms and processes. *Earth Surface Processes and Landforms* 41: 701–710. DOI: 10.1002/esp.3893
- Gesch D, Oimoen M, Greenlee S, Nelson C, Steuck M, Tyler D. 2002. The national elevation dataset. *Photogrammetric engineering and remote sensing* 68: 5–32.
- Gilbert GK. 1917. *Hydraulic-mining debris in the Sierra Nevada* . United States Geological Survey [online] Available from: <https://doi.org/10.3133/pp105> (Accessed 26 September 2019)
- Gilbert JT, Macfarlane WW, Wheaton JM. 2016. The Valley Bottom Extraction Tool (V-BET): A GIS tool for delineating valley bottoms across entire drainage networks. *Computers & Geosciences* 97: 1–14. DOI: 10.1016/j.cageo.2016.07.014
- Gomi T, Sidle RC, Richardson JS. 2002. Understanding Processes and Downstream Linkages of Headwater Systems. *BioScience* 52: 905-916. DOI: 10.1641/0006-3568(2002)052[0905:UPADLO]2.0.CO;2
- Graf WL. 1988. *Fluvial processes in dryland rivers* . Springer-Verlag: Berlin [online] Available from: [https://scholar.google.com/scholar\\_lookup?title=Fluvial%20processes%20in%20dryland%20rivers&author=W.L.%20Graf&publication\\_year=1988](https://scholar.google.com/scholar_lookup?title=Fluvial%20processes%20in%20dryland%20rivers&author=W.L.%20Graf&publication_year=1988) (Accessed 4 December 2018)
- Grams PE, Schmidt JC. 2002. Streamflow regulation and multi-level flood plain formation: channel narrowing on the aggrading Green River in the eastern Uinta Mountains, Colorado and Utah. *Geomorphology* 44: 337–360. DOI: 10.1016/S0169-555X(01)00182-9
- Grant GE, O'Connor JE. 2003. A peculiar river: geology, geomorphology, and hydrology of the Deschutes River, Oregon . *American Geophysical Union*

- Grant GE, Swanson FJ. 1995. Morphology and processes of valley floors in mountain streams, western Cascades, Oregon. *Geophysical Monograph-American Geophysical Union* 89: 83–83.
- Grant GE, Swanson FJ, Wolman MG. 1990. Pattern and origin of stepped-bed morphology in high-gradient streams, Western Cascades, Oregon. *GSA Bulletin* 102: 340–352. DOI: 10.1130/0016-7606(1990)102<0340:PAOOSB>2.3.CO;2
- Grill G , Lehner B, Thieme M, Geenen B, Tickner D, Antonelli F, Babu S, Borrelli P, Cheng L, Crochetiere H, Macedo HE, Filgueiras R, Goichot M, Higgins J, Hogan Z, Lip B, McClain ME, Meng J, Mulligan M, Nilsson C, Olden JD, Opperman JJ, Petry P, Liermann CR, Sáenz L, Salinas-Rodríguez S, Schelle P, Schmitt RJP, Snider J, Tan F, Tockner K, Valdujo PH, van Soesbergen A, Zarfle C. 2019. Mapping the world’s free-flowing rivers. *Nature* 569: 215–221. DOI: 10.1038/s41586-019-1111-9
- Guillon H, Byrne CF, Lane BA, Solis SS, Pasternack GB. 2020. Machine Learning Predicts Reach-Scale Channel Types From Coarse-Scale Geospatial Data in a Large River Basin. *Water Resources Research* 56: e2019WR026691, 1-22. DOI: 10.1029/2019WR026691
- Guinn JM. 1890. Exceptional years: a history of California floods and drought. *Historical Society of Southern California, Los Angeles* (1890) 1: 33–39. DOI: 10.2307/41167825
- Gurnell AM. 2014. Plants as river system engineers. *Earth Surface Processes and Landforms* 39: 4–25. DOI: 10.1002/esp.3397
- Gurnell AM, Rinaldi M, Belletti B, Bizzi S, Blamauer B, Braca G, Buijse AD, Bussettini M, Camenen B, Comiti F, Demarchi L, García de Jalón D, González del Tánago M, Grabowski RC, Gunn IDM, Habersack H, Hendriks D, Henshaw AJ, Klösch M, Lastoria B, Latapie A, Marcinkowski P. 2016. A multi-scale hierarchical framework for developing understanding of river behaviour to support river management. *Aquatic Sciences* 78: 1–16. DOI: 10.1007/s00027-015-0424-5
- Hack JT. 1960. Interpretation of erosional topography in humid temperate regions. *American Journal of Science* 258-A: 80–97.
- Harvey AM. 1991. The influence of sediment supply on the channel morphology of upland streams: Howgill Fells, Northwest England. *Earth Surface Processes and Landforms* 16: 675–684. DOI: 10.1002/esp.3290160711
- Hauer C, Pulg U. 2018. The non-fluvial nature of Western Norwegian rivers and the implications for channel patterns and sediment composition. *CATENA* 171: 83–98. DOI: 10.1016/j.catena.2018.06.025
- Heitmuller FT, Hudson PF, Asquith WH. 2015. Lithologic and hydrologic controls of mixed alluvial–bedrock channels in flood-prone fluvial systems: Bankfull and macrochannels in the Llano River watershed, central Texas, USA. *Geomorphology* 232: 1–19. DOI: 10.1016/j.geomorph.2014.12.033
- Hooke RLeB. 1967. Processes on Arid-Region Alluvial Fans. *The Journal of Geology* 75: 438–460. DOI: 10.1086/627271
- Huang HQ, Chang HH, Nanson GC. 2004. Minimum energy as the general form of critical flow and maximum flow efficiency and for explaining variations in river channel pattern. *Water Resources Research* 40: W04502, 1-13. DOI: 10.1029/2003WR002539 [online] Available from: <http://doi.wiley.com/10.1029/2003WR002539> (Accessed 26 February 2019)

- Hubert L, Arabie P. 1985. Comparing partitions. *Journal of Classification* 2: 193–218. DOI: 10.1007/BF01908075
- James LA. 1991. Incision and morphologic evolution of an alluvial channel recovering from hydraulic mining sediment. *Geological Society of America Bulletin* 103: 723–736.
- Kasprak A, Hough-Snee N, Beechie T, Bouwes N, Brierley G, Camp R, Fryirs K, Imaki H, Jensen M, O'Brien G, Rosgen D, Wheaton J. 2016. The Blurred Line between Form and Process: A Comparison of Stream Channel Classification Frameworks. *PLOS ONE* 11: e0150293, 1-31. DOI: 10.1371/journal.pone.0150293
- Kassambara A. 2019. rstatix: Pipe-Friendly Framework for Basic Statistical Tests. [online] Available from: <https://CRAN.R-project.org/package=rstatix>
- Knighton AD. 1980. Longitudinal changes in size and sorting of stream-bed material in four English rivers. *GSA Bulletin* 91: 55–62. DOI: 10.1130/0016-7606(1980)91<55:LCISAS>2.0.CO;2
- Knighton D. 1998. *Fluvial Forms and Processes: A New Perspective*. Routledge: New York, NY
- Kondolf GM. 1997. Hungry Water: Effects of Dams and Gravel Mining on River Channels. *Environmental Management* 21: 533–551. DOI: 10.1007/s002679900048
- Kondolf GM, Piégay H, Schmitt L, Montgomery DR. 2016. Geomorphic classification of rivers and streams. In *Tools in Fluvial Geomorphology*, Kondolf GM and Piégay H (eds). John Wiley & Sons, Ltd; 133–158. [online] Available from: <http://onlinelibrary.wiley.com/doi/10.1002/9781118648551.ch7/summary> (Accessed 23 January 2018)
- Lane BA, Dahlke HE, Pasternack GB, Sandoval-Solis S. 2017a. Revealing the Diversity of Natural Hydrologic Regimes in California with Relevance for Environmental Flows Applications. *JAWRA Journal of the American Water Resources Association* 53: 411–430. DOI: 10.1111/1752-1688.12504
- Lane BA, Pasternack GB, Dahlke HE, Sandoval-Solis S. 2017b. The role of topographic variability in river channel classification. *Progress in Physical Geography* 41: 570-600. DOI: 10.1177/0309133317718133
- Lane BA, Pasternack GB, Sandoval-Solis S. 2018a. Integrated analysis of flow, form, and function for river management and design testing. *Ecohydrology* 11: e1969, 1-15. DOI: 10.1002/eco.1969 [online] Available from: <https://onlinelibrary.wiley.com/doi/abs/10.1002/eco.1969> (Accessed 9 April 2018)
- Lane BA, Sandoval-Solis S, Stein ED, Yarnell SM, Pasternack GB, Dahlke HE. 2018b. Beyond Metrics? The Role of Hydrologic Baseline Archetypes in Environmental Water Management. *Environmental Management* 62: 678-693. DOI: 10.1007/s00267-018-1077-7 [online] Available from: <http://link.springer.com/10.1007/s00267-018-1077-7> (Accessed 2 July 2018)
- Lane EW. 1954. The importance of fluvial morphology in hydraulic engineering. Hydraulic Laboratory Report. U.S. Department of Interior - Bureau of Reclamation
- Lane SN. 1995. The Dynamics of Dynamic River Channels. *Geography* 80: 147–162.
- Langbein WB, Leopold LB. 1964. Quasi-equilibrium states in channel morphology. *American Journal of Science* 262: 782–794. DOI: 10.2475/ajs.262.6.782
- Leopold LB, Maddock T. 1953. The Hydraulic Geometry of Stream Channels and Some Physiographic Implications

- Leopold LB, Wolman MG. 1957. River channel patterns: Braided, meandering, and straight . USGS Numbered Series. U.S. Government Printing Office: Washington, D.C. [online] Available from: <http://pubs.er.usgs.gov/publication/pp282B> (Accessed 9 November 2018)
- MacWilliams ML, Wheaton JM, Pasternack GB, Street RL, Kitanidis PK. 2006. Flow convergence routing hypothesis for pool-riffle maintenance in alluvial rivers. *Water Resources Research* 42: W10427, 1-21. DOI: 10.1029/2005WR004391
- Makaske B. 2001. Anastomosing rivers: a review of their classification, origin and sedimentary products. *Earth-Science Reviews* 53: 149–196. DOI: 10.1016/S0012-8252(00)00038-6
- McClymont AF, Hayashi M, Bentley LR, Muir D, Ernst E. 2010. Groundwater flow and storage within an alpine meadow-talus complex. *Hydrology and Earth System Sciences* 14: 859–872. DOI: 10.5194/hess-14-859-2010
- McKay L, Bondelid T, Dewald T, Johnston J, Moore R, Rea A. 2012. NHDPlus version 2: user guide. US Environmental Protection Agency
- Melis TS, Korman J, Kennedy TA. 2012. Abiotic & Biotic Responses of the Colorado River to Controlled Floods at Glen Canyon Dam, Arizona, Usa. *River Research and Applications* 28: 764–776. DOI: 10.1002/rra.1503
- Miller MC, McCAYE IN, Komar PD. 1977. Threshold of sediment motion under unidirectional currents. *Sedimentology* 24: 507–527. DOI: 10.1111/j.1365-3091.1977.tb00136.x
- Milliman JD, Syvitski JP. 1992. Geomorphic/Tectonic Control of Sediment Discharge to the Ocean: The Importance of Small Mountainous Rivers. *The Journal of Geology* 100: 525–544.
- Moir HJ, Pasternack GB. 2010. Substrate requirements of spawning Chinook salmon (*Oncorhynchus tshawytscha*) are dependent on local channel hydraulics. *River Research and Applications* 26: 456–468. DOI: 10.1002/rra.1292
- Montgomery DR. 1999. Process Domains and the River Continuum. *JAWRA Journal of the American Water Resources Association* 35: 397–410. DOI: 10.1111/j.1752-1688.1999.tb03598.x
- Montgomery DR, Abbe TB, Buffington JM, Peterson NP, Schmidt KM, Stock JD. 1996. Distribution of bedrock and alluvial channels in forested mountain drainage basins. *Nature* 381: 587–589. DOI: 10.1038/381587a0
- Montgomery DR, Buffington JM. 1997. Channel-reach morphology in mountain drainage basins. *Geological Society of America Bulletin* 109: 596–611.
- Montgomery DR, Buffington JM. 1998. Channel processes, classification, and response. *River Ecology and Management: Lessons from the Pacific Coastal Ecoregion*, RJ Naiman and RE Bilby (Editors). Springer-Verlag, New York, New York : 13–42.
- Mount JF. 1995. California rivers and streams: the conflict between fluvial process and land use . Univ of California Press
- Murtagh F, Legendre P. 2014a. Ward’s Hierarchical Agglomerative Clustering Method: Which Algorithms Implement Ward’s Criterion? *Journal of Classification* 31: 274–295. DOI: 10.1007/s00357-014-9161-z
- Murtagh F, Legendre P. 2014b. Ward’s Hierarchical Clustering Method: Clustering Criterion and Agglomerative Algorithm. *Journal of Classification* 31: 274–295. DOI: 10.1007/s00357-014-9161-z

- Neeson TM, Gorman AM, Whiting PJ, Koonce JF. 2008. Factors Affecting Accuracy of Stream Channel Slope Estimates Derived from Geographical Information Systems. *North American Journal of Fisheries Management* 28: 722–732. DOI: 10.1577/M05-127.1
- O'Brien GR, Wheaton JM, Fryirs K, Macfarlane WW, Brierley G, Whitehead K, Gilbert J, Volk C. 2019. Mapping Valley Bottom Confinement at the Network Scale. *Earth Surface Processes and Landforms* 44: 1828-1845. DOI: 10.1002/esp.4615 [online] Available from: <https://onlinelibrary.wiley.com/doi/abs/10.1002/esp.4615> (Accessed 28 March 2019)
- Ode PR. 2007. Standard operating procedures for collecting benthic macroinvertebrate samples and associated physical and chemical data for ambient bioassessments in California. *Surface Water Ambient Monitoring Program (SWAMP) Bioassessment SOP 1: California State Water Resources Control Board: Sacramento, CA.*
- Omernik JM. 1987. Ecoregions of the Conterminous United States. *Annals of the Association of American Geographers* 77: 118–125. DOI: 10.1111/j.1467-8306.1987.tb00149.x
- Palmer T. 2012. *Field guide to California rivers* . Univ of California Press
- Park CC. 1977. World-wide variations in hydraulic geometry exponents of stream channels: An analysis and some observations. *Journal of Hydrology* 33: 133–146. DOI: 10.1016/0022-1694(77)90103-2
- Parker G. 1979. Hydraulic geometry of active gravel rivers. *Journal of the Hydraulics Division* 105: 1185–1201.
- Parrett C, Veilleux A, Stedinger JR, Barth NA, Knifong DL, Ferris JC. 2011. Regional skew for California, and flood frequency for selected sites in the Sacramento-San Joaquin River Basin, based on data through water year 2006 . U. S. Geological Survey
- Pasternack GB, Baig D, Weber MD, Brown RA. 2018a. Hierarchically nested river landform sequences. Part 1: Theory. *Earth Surface Processes and Landforms* 43: 2510–2518. DOI: 10.1002/esp.4411
- Pasternack GB, Baig D, Weber MD, Brown RA. 2018b. Hierarchically nested river landform sequences. Part 2: Bankfull channel morphodynamics governed by valley nesting structure. *Earth Surface Processes and Landforms* 43: 2519–2532. DOI: 10.1002/esp.4410
- Paustian SJ. 2010. *A Channel Type Users Guide for the Tongass National Forest, Southeast Alaska* . Technical Report. USDA Forest Service, Region 10 [online] Available from: <https://dSPACE.nmc.edu/handle/11045/20008> (Accessed 22 September 2017)
- Pfeiffer AM, Finnegan NJ. 2018. Regional Variation in Gravel Riverbed Mobility, Controlled by Hydrologic Regime and Sediment Supply. *Geophysical Research Letters* 45: 3097–3106. DOI: 10.1002/2017GL076747
- Pfeiffer AM, Finnegan NJ, Willenbring JK. 2017. Sediment supply controls equilibrium channel geometry in gravel rivers. *Proceedings of the National Academy of Sciences* 114: 3346–3351. DOI: 10.1073/pnas.1612907114
- Phillips CB, Jerolmack DJ. 2016. Self-organization of river channels as a critical filter on climate signals. *Science* 352: 694–697. DOI: 10.1126/science.aad3348
- Pitlick J, Cress R. 2002. Downstream changes in the channel geometry of a large gravel bed river. *Water Resources Research* 38: 34-1-34–11. DOI: 10.1029/2001WR000898



- Pizzuto JE. 1994. Channel adjustments to changing discharges, Powder River, Montana. *Geological Society of America Bulletin* 106: 1494–1501. DOI: 10.1130/0016-7606(1994)106<1494:CATCDP>2.3.CO;2
- Poff NL Poff NL, Richter BD, Arthington AH, Bunn SE, Naiman RJ, Kendy E, Acreman M, Apse C, Bledsoe BP, Free man MC, Henriksen J, Jacobson RB, Kennen JG, Merritt DM, O’Keeffe JH, Olden JD, Rogers K, Tharme R E, Warner A. 2010. The ecological limits of hydrologic alteration (ELOHA): a new framework for developing regional environmental flow standards. *Freshwater Biology* 55: 147–170.
- Poff NL, Allan JD, Bain MB, Karr JR, Presteggaard KL, Richter BD, Sparks RE, Stromberg JC. 1997. The natural flow regime. *BioScience* 47: 769–784.
- Poff NL, Bledsoe BP, Cuhaciyar CO. 2006. Hydrologic variation with land use across the contiguous United States: Geomorphic and ecological consequences for stream ecosystems. *Geomorphology* 79: 264–285. DOI: 10.1016/j.geomorph.2006.06.032
- Polvi LE, Wohl EE, Merritt DM. 2011. Geomorphic and process domain controls on riparian zones in the Colorado Front Range. *Geomorphology* 125: 504–516. DOI: 10.1016/j.geomorph.2010.10.012
- PRISM Climate Group. 2007. Oregon State University [online] Available from: <http://prism.oregonstate.edu>
- R Core Team. 2017. R: A Language and Environment for Statistical Computing . R Foundation for Statistical Computing: Vienna, Austria [online] Available from: <https://www.R-project.org/>
- Rathburn SL, Shahverdian SM, Ryan SE. 2018. Post-disturbance sediment recovery: Implications for watershed resilience. *Geomorphology* 305: 61–75. DOI: 10.1016/j.geomorph.2017.08.039
- Reid I, Laronne JB. 1995. Bed Load Sediment Transport in an Ephemeral Stream and a Comparison with Seasonal and Perennial Counterparts. *Water Resources Research* 31: 773–781. DOI: 10.1029/94WR02233
- Richards KS. 1977. Channel and flow geometry: a geomorphological perspective. *Progress in Physical Geography: Earth and Environment* 1: 65–102. DOI: 10.1177/030913337700100105
- Ritter DF, Kochel RC, Miller JR, Miller JR. 1995. *Process geomorphology* . Wm. C. Brown Dubuque, IA
- Rosgen DL. 1994. A classification of natural rivers. *CATENA* 22: 169–199. DOI: 10.1016/0341-8162(94)90001-9
- Rosgen DL. 1996. *Applied river morphology*. Wildland Hydrology: Pagosa Springs.
- Schmitt L, Maire G, Nobelis P, Humbert J. 2007. Quantitative morphodynamic typology of rivers: a methodological study based on the French Upper Rhine basin. *Earth Surface Processes and Landforms* 32: 1726–1746. DOI: 10.1002/esp.1596
- Schumm SA. 1977. *The fluvial system*. Wiley: New York
- Shields A. 1936. *Application of similarity principles and turbulence research to bed-load movement*
- Sholtes JS, Yochum SE, Scott JA, Bledsoe BP. 2018. Longitudinal variability of geomorphic response to floods: Geomorphic response to floods. *Earth Surface Processes and Landforms* 43: 3099–3113. DOI: 10.1002/esp.4472 [online] Available from: <http://doi.wiley.com/10.1002/esp.4472> (Accessed 24 September 2018)

- Singer MB. 2007. The influence of major dams on hydrology through the drainage network of the Sacramento River basin, California. *River Research and Applications* 23: 55–72. DOI: 10.1002/rra.968
- Sloan J, Miller JR, Lancaster N. 2001. Response and recovery of the Eel River, California, and its tributaries to floods in 1955, 1964, and 1997. *Geomorphology* 36: 129–154. DOI: 10.1016/S0169-555X(00)00037-4
- Snow RS. 1989. Fractal sinuosity of stream channels. *Pure and applied geophysics* 131: 99–109.
- Strahler AN. 1957. Quantitative analysis of watershed geomorphology. *Eos, Transactions American Geophysical Union* 38: 913–920. DOI: 10.1029/TR038i006p00913
- Sutfin NA, Shaw JR, Wohl EE, Cooper DJ. 2014. A geomorphic classification of ephemeral channels in a mountainous, arid region, southwestern Arizona, USA. *Geomorphology* 221: 164–175. DOI: 10.1016/j.geomorph.2014.06.005
- Swanson BJ, Meyer GA, Coonrod JE. 2011. Historical channel narrowing along the Rio Grande near Albuquerque, New Mexico in response to peak discharge reductions and engineering: magnitude and uncertainty of change from air photo measurements. *Earth Surface Processes and Landforms* 36: 885–900. DOI: 10.1002/esp.2119
- Thanapakpawin P, Richey J, Thomas D, Rodda S, Campbell B, Logsdon M. 2007. Effects of landuse change on the hydrologic regime of the Mae Chaem river basin, NW Thailand. *Journal of Hydrology* 334: 215–230. DOI: 10.1016/j.jhydrol.2006.10.012
- Therneau TM, Atkinson EJ. 2018. rpart: Recursive Partitioning and Regression Trees. . Mayo Foundation [online] Available from: <https://CRAN.R-project.org/package=rpart>
- Thompson A. 1986. Secondary flows and the pool-riffle unit: A case study of the processes of meander development. *Earth Surface Processes and Landforms* 11: 631–641. DOI: 10.1002/esp.3290110606
- Tooth S. 2000. Process, form and change in dryland rivers: a review of recent research. *Earth-Science Reviews* 51: 67–107. DOI: 10.1016/S0012-8252(00)00014-3
- Tooth S, Nanson GC. 2004. Forms and processes of two highly contrasting rivers in arid central Australia, and the implications for channel-pattern discrimination and prediction. *GSA Bulletin* 116: 802–816. DOI: 10.1130/B25308.1
- USGS. 2016. GAP/LANDFIRE National Terrestrial Ecosystems 2011. DOI: 10.5066/f7zs2tm0 [online] Available from: <https://www.sciencebase.gov/catalog/item/573cc51be4b0dae0d5e4b0c5> (Accessed 30 September 2019)
- Ward JHJ. 1963. Hierarchical Grouping to Optimize an Objective Function. *Journal of the American Statistical Association* 58: 236–244. DOI: 10.1080/01621459.1963.10500845
- White JQ, Pasternack GB, Moir HJ. 2010. Valley width variation influences riffle–pool location and persistence on a rapidly incising gravel-bed river. *Geomorphology* 121: 206–221. DOI: 10.1016/j.geomorph.2010.04.012
- Wohl E, Bledsoe BP, Jacobson RB, Poff NL, Rathburn SL, Walters DM, Wilcox AC. 2015. The Natural Sediment Regime in Rivers: Broadening the Foundation for Ecosystem Management. *BioScience* 65: 358–371. DOI: 10.1093/biosci/biv002
- Wohl EE. 2000. Mountain rivers. American Geophysical Union: Washington DC.

- Wohl EE. 2010. A brief review of the process domain concept and its application to quantifying sediment dynamics in bedrock canyons. *Terra Nova* 22: 411–416. DOI: 10.1111/j.1365-3121.2010.00950.x
- Wohl EE. 2013. The complexity of the real world in the context of the field tradition in geomorphology. *Geomorphology* 200: 50–58. DOI: 10.1016/j.geomorph.2012.12.016
- Wohl EE, Merritt DM. 2008. Reach-scale channel geometry of mountain streams. *Geomorphology* 93: 168–185. DOI: 10.1016/j.geomorph.2007.02.014
- Wohl EE, Pearthree PP. 1991. Debris flows as geomorphic agents in the Huachuca Mountains of southeastern Arizona. *Geomorphology* 4: 273–292. DOI: 10.1016/0169-555X(91)90010-8
- Wolman MG. 1954. A method of sampling coarse river-bed material. *Eos, Transactions American Geophysical Union* 35: 951–956. DOI: 10.1029/TR035i006p00951
- Wright SA, Schoellhamer DH. 2004. Trends in the Sediment Yield of the Sacramento River, California, 1957–2001. *San Francisco Estuary and Watershed Science* 2: 1-14. DOI: 10.15447/sfews.2004v2iss2art2 [online] Available from: <https://escholarship.org/uc/item/891144f4> (Accessed 7 February 2020)
- Wyrick JR, Pasternack GB. 2014. Geospatial organization of fluvial landforms in a gravel–cobble river: Beyond the riffle–pool couplet. *Geomorphology* 213: 48–65. DOI: 10.1016/j.geomorph.2013.12.040
- Yang CT, Song CCS, Woldenberg MJ. 1981. Hydraulic geometry and minimum rate of energy dissipation. *Water Resources Research* 17: 1014–1018. DOI: 10.1029/WR017i004p01014
- Yang D, Kane DL, Hinzman LD, Zhang X, Zhang T, Ye H. 2002. Siberian Lena River hydrologic regime and recent change. *Journal of Geophysical Research: Atmospheres* 107: 4694, 1-10. DOI: 10.1029/2002JD002542
- Yochum SE, Sholtes JS, Scott JA, Bledsoe BP. 2017. Stream power framework for predicting geomorphic change: The 2013 Colorado Front Range flood. *Geomorphology* 292: 178–192.
- Zimmermann A, Church M, Hassan MA. 2010. Step-pool stability: Testing the jammed state hypothesis. *Journal of Geophysical Research: Earth Surface* 115: F02008, 1-16. DOI: 10.1029/2009JF001365 [online] Available from: <http://doi.wiley.com/10.1029/2009JF001365> (Accessed 27 August 2018)

## Acknowledgements

This research was supported by the California State Water Resources Control Board under grant number 16-062-300. We also acknowledge the USDA National Institute of Food and Agriculture, Hatch project numbers #CA-D-LAW-7034-H and CA-D-LAW-2243-H. Finally, we would like to thank Brianna Ordnung and John Deane for their roles in field data collection.

## Data Availability Statement

The geomorphic data that support the findings of this study are available in the supplementary material of this article. The hydrologic data that support the findings of this study are available from references provided within the methodology of this article or, where adapted, are available from the corresponding author on reasonable request.

## **Conflict of Interest**

The authors have no conflict of interest to declare.

**Supplementary information to ‘Reach-scale bankfull channel types  
can exist independently of catchment hydrology’**

## Summary statistics of reach-scale sites and channel types

Table S1. Statistical measure of site attributes considered for classification of reach-scale channel types.

	Ac (km <sup>2</sup> )	s	d (m)	w (m)	w/d	d/D50	CVd	CVw	k	D50 (mm)	D84 (mm)	Cv (m)
Minimum	1	0.000	0.2	1.3	2.9	0	0.03	0.00	1.01	2	2	1
Maximum	7498	0.143	3.2	47.0	47.1	1285	0.78	0.78	2.20	5000	5000	5000
Range	7497	0.143	3.0	45.7	44.2	1285	0.75	0.78	1.19	4998	4998	4999
Mean	261	0.020	1.0	11.0	12.6	58	0.27	0.25	1.22	249	1733	871
Median	53	0.014	0.9	9.4	10.6	11	0.24	0.24	1.20	70	405	109
Standard Deviation	901	0.020	0.5	6.7	7.1	143	0.13	0.11	0.16	655	2081	1455

Table S2. Median channel attributes considered for classification of reach-scale channel types.

Channel Type	Ac (km <sup>2</sup> )	s	d (m)	w (m)	w/d	d/D50	CVd	CVw	k	D50 (mm)	D84 (mm)	Cv (m)
1	7466	0.004	0.9	16.0	16.8	5	0.49	0.23	1.10	564	5000	1202
2	84	0.042	1.0	11.0	11.0	5	0.20	0.26	1.20	250	2500	28
3	100	0.014	1.1	10.9	10.8	6	0.23	0.20	1.20	190	5000	46
4	31	0.018	0.9	6.7	7.3	6	0.34	0.32	1.19	128	5000	23
5	30	0.020	0.7	6.6	9.4	10	0.20	0.18	1.12	57	200	62
6	32	0.012	0.7	6.8	8.6	23	0.23	0.32	1.20	40	95	598
7	164	0.014	1.3	16.2	13.4	16	0.19	0.17	1.23	87	380	114
8	54	0.006	0.7	11.6	16.8	28	0.42	0.25	1.19	27	130	104
9	74	0.007	1.0	8.1	8.5	65	0.23	0.24	1.15	11	45	4688
10	170	0.009	1.1	17.8	20.5	35	0.30	0.26	1.14	28	64	2868

## Valley confinement-sediment size relationships

Within the main text of the associated manuscript, statistical relationships between valley confinement distances and sediment size are documented. Figure S1 displays the log-log regressions associated with the statistical metrics in the manuscript.

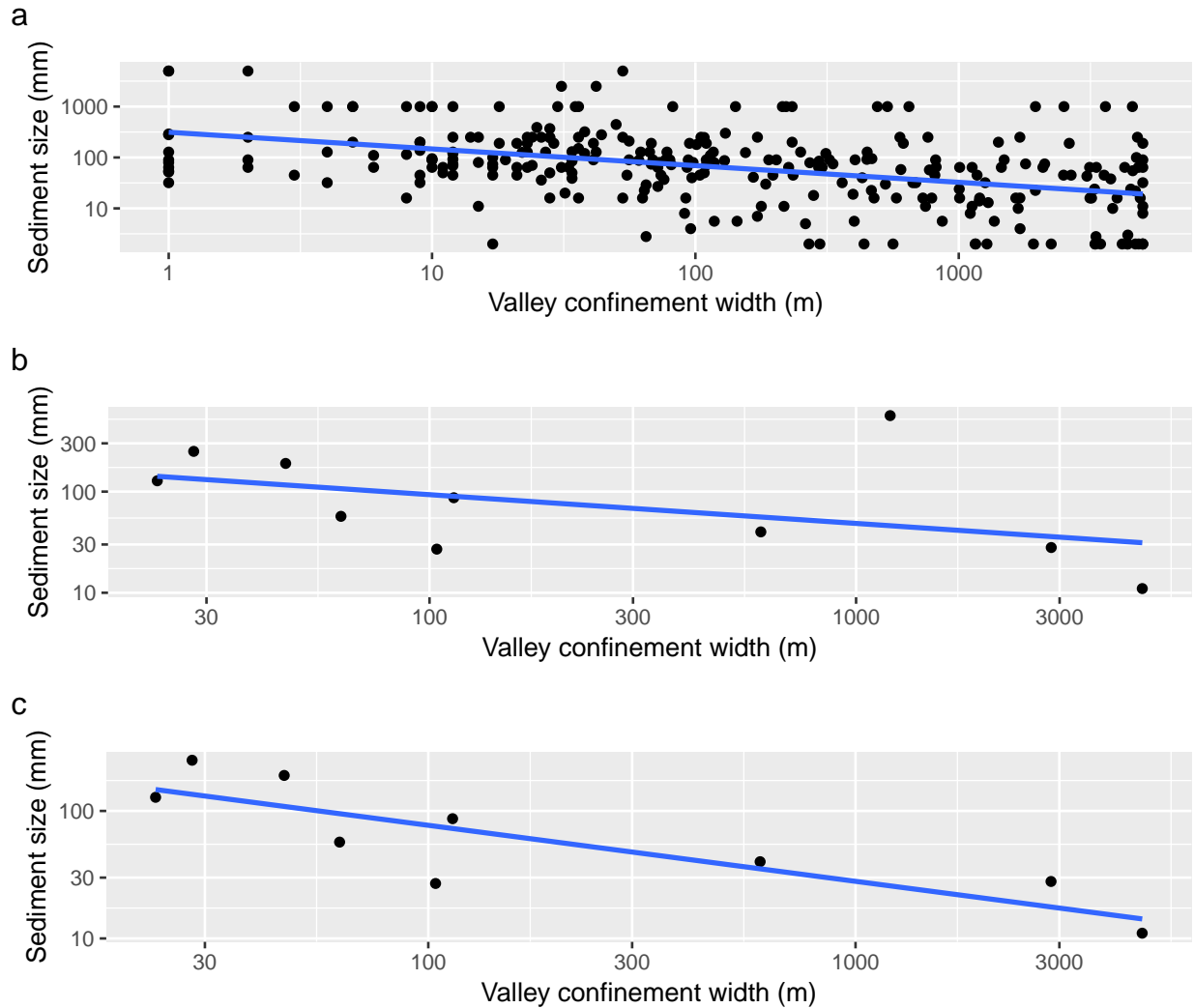


Figure S1. Relationships between valley confinement and sediment size for a) values at all 288 sites, b) median values at all ten channel types, and c) median values for channel types 2 through 10.

## Calculation of site-specific flood discharge

In order to compare reach-scale channel types to flood magnitudes, flows for 2-, 5-, 10-, 25-, and 50-year recurrence interval flood events were estimated at each survey site. These estimations were developed based on the combination of USGS estimations of flow at 84 reference gauges with a minimum of 30-years of flow data and streams binned by defining annual hydrologic regime [Parrett et al. 2011; Lane et al. 2018]. Gauges were binned according to their spatial overlap with binned streams. Contributing area at each gauge location was also estimated using data from 10-m DEM and streamlines from the National Hydrography Dataset Plus Version 2. The binning of gauges by hydrologic regime resulted in notable and consistent differences between gauges in different hydrologic settings, especially high-elevation, low-elevation (HLP) gauges (Fig. S4).

Given the differences in gauge discharge estimates for each of the annual hydrologic regimes,

estimation of discharges for all survey sites were also dependent upon the annual hydrologic regime in which it is located. Best-fit power functions were fit to the log-log drainage area-discharge relationships of the following form:

$$Q = kA^m$$

where  $Q$  is discharge,  $A$  is contributing drainage area, and  $k$  and  $m$  are numerical constants. Calculated discharges for each site were then used in the comparison of reach-scale channel types with flood magnitude and dimensionless flood magnitude. As discussed in the main text, estimates of flood magnitude for a 10-year recurrence interval were used in the statistical hydrogeomorphic analysis because statistical results were maximized or near maximum. The fit parameters for each of the annual hydrologic regimes at the 10-year recurrence interval are documented in Table S2.

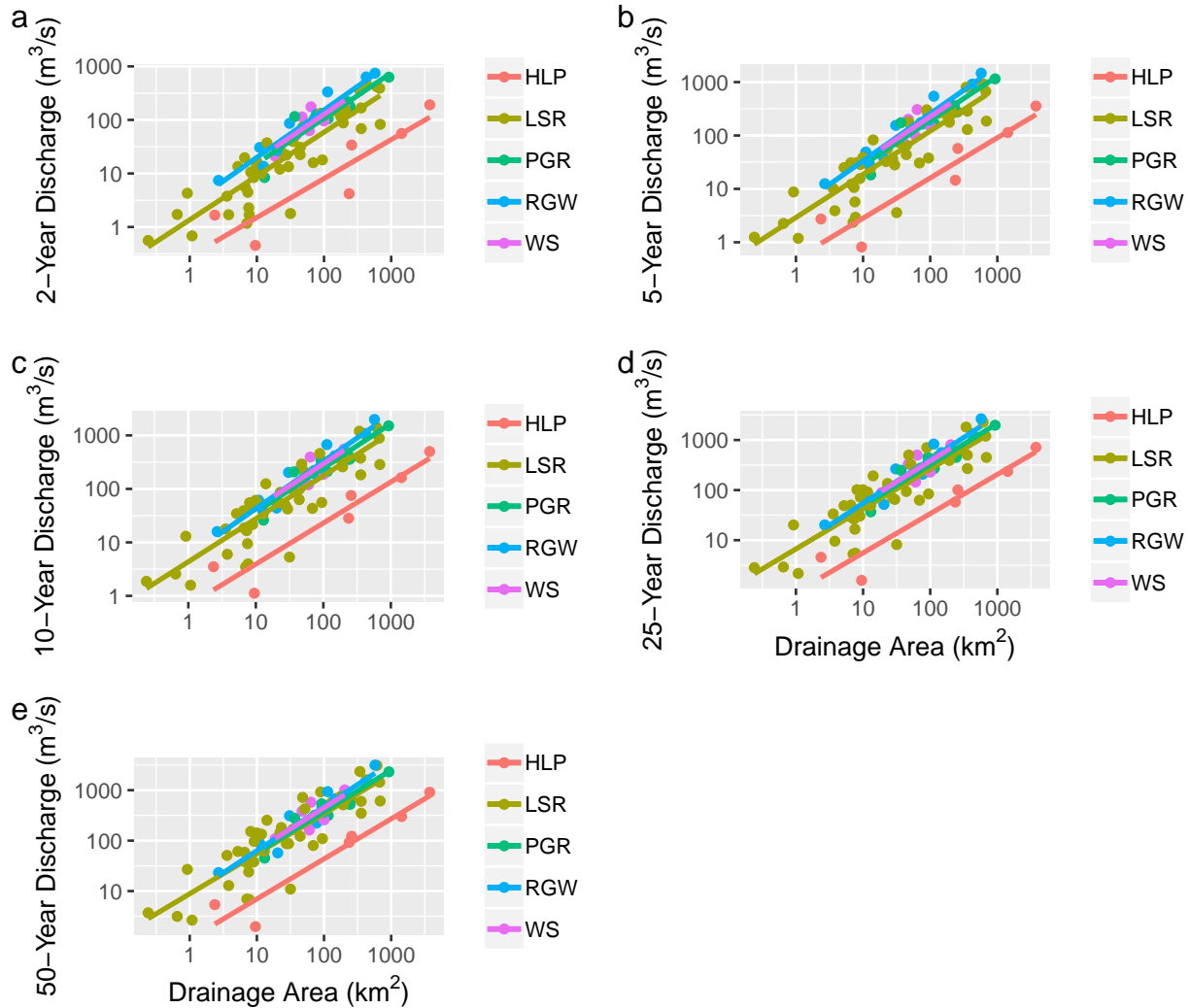


Figure S2. Area-discharge flood regressions for five hydrologic regions within the Sacramento River basin developed from USGS calculated flood magnitudes at reference gauges.



Table S3. Adjusted r-squared values for all log-transformed linear regressions in Figure S2 ( $p < 0.05$  for all regressions).

	HLP	LSR	PGR	RGW	WS
2-year	0.76	0.79	0.80	0.93	0.62
5-year	0.83	0.78	0.85	0.93	0.61
10-year	0.86	0.77	0.86	0.93	0.60
25-year	0.88	0.76	0.88	0.92	0.58
50-year	0.89	0.75	0.89	0.91	0.56

## Assessing site distances and variance in multiple dimensions

Informative analysis of multivariate distances between survey sites was informed by non-metric multidimensional scaling (NMDS) to visualize site distances [Anderson et al., 2001; Clarke, 1993; Kruskal, 1964], and principal component analysis (PCA) was used to understand what reach-scale attributes explained the most variance between sites. NMDS was conducted using the metaMDS function (vegan package) and calculated based upon Euclidean distance between rescaled attributes [Oksanen et al., 2019]. The PCA used the ‘precomp’ function (stats package) and was calculated based on rescaled attributes. In the presented results, the PCA vectors are plotted on top of the NMDS ordination as the metaMDS function automatically rotates the NMDS axes to those associated with the PCA analysis. The results helped to understand how the study sites and reach-scale attributes were related within multivariate space, but ultimately did not define the reach-scale classification.

Sediment size and valley confinement were identified as the most influential channel attributes in assessing distances between sites in multivariate space. The two-dimensional non-metric multidimensional scaling (NMDS) stress was 0.141 (Fig. S2). When analyzed in three-dimensions, the NMDS stress drops to 0.097, representative of a ‘good’ ordination [Clarke, 1993], with a non-metric coefficient of determination of 0.991 between observed dissimilarity and ordination distance (Fig. S3). The first and second principle component axes (PCAs) resulting from the NMDS ordination explained 45 and 19% of the variance in the data, respectively. Loadings of 0.94 for D84 and 0.91 for Cv for PCA-1 and PCA-2, respectively. These loading values indicate that these two variables had the strongest influence on multivariate variance between sites as compared to other independent variables.

Final channel types were made up of 4 to 45 sites. Clusters with a small number of sites were avoided, as outliers were expected to represent site-specific differences rather than larger basin trends. However, it was ultimately the uniqueness of cluster attributes that drove final classifications. For example, there are only four sites in channel type 1 (Fig. 5b), but the sites are clustered closely to one another and do not exhibit similarities to other channel types. That differentiates the grouping from the concept of a statistical outlier. An outlier is an individual sample far away from a grouping, while a set of outliers is a number of such randomly distributed individual samples probabilistically unlikely to present as a tight grouping. Though a set of outliers could theoretically group by random chance, geomorphic interpretation of any grouping can evaluate whether a cluster meets the concept of a channel type or just a random statistical artifact. In addition, Dunn’s Tests aided in assessing uniqueness.

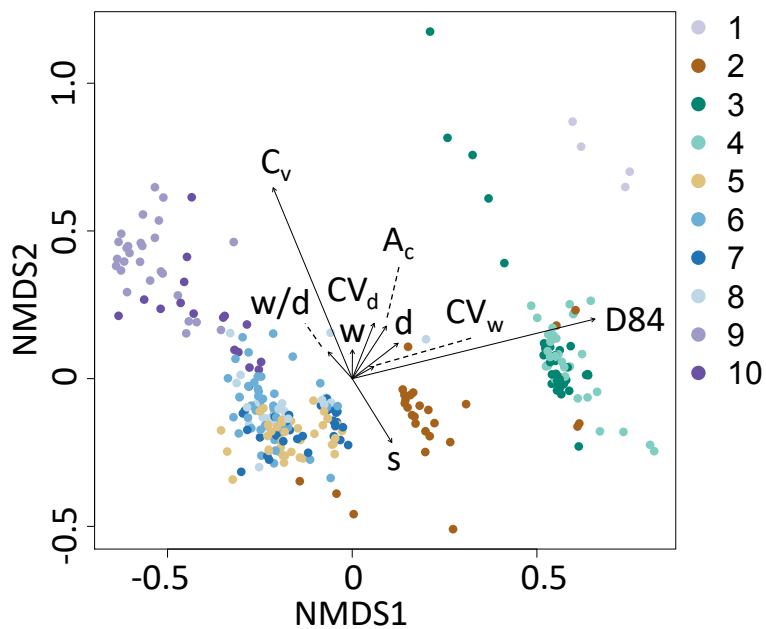


Figure S3. Site data plotted in the first two NMDS dimensions. The NMDS solution is oriented with the first two PCAs. Therefore, vectors represent the influence of hydrogeomorphic site attributes on the variance between sites. The longer the vector, the more variance is explained by the attribute.

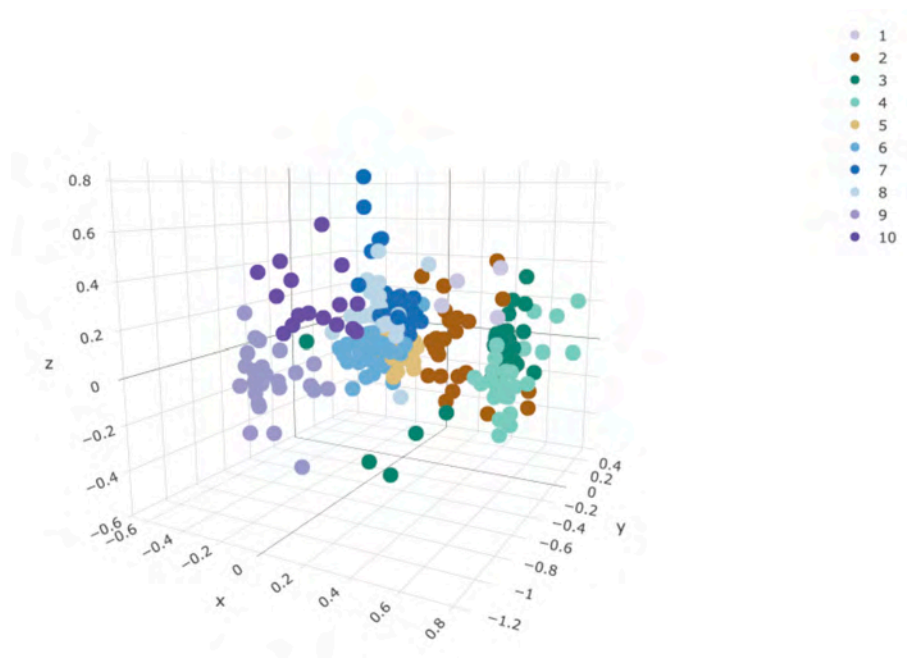


Figure S4. A three-dimensional representation of the NMDS organization of sites.

## Accuracy of reach-scale channel types

Cross-validation of the classification tree was conducted in order to better understand the stability of the multivariate classification. The cross-validation metric is included in the manuscript as it provides the most simple representation of the classification. Two other methods were used to conduct tests of the ability of the classification to predict against unseen data: a multinomial logistic regression implemented with an artificial neural-network (ANN) approach and a generalized linear model (GLM) approach. The ANN approach was implemented using the “multinom” function (‘nnet’ package) and the GLM approach used the “glmnet” function (‘glmnet’ package). Both functions were run 100 times with a 70-30 percent random subsetting of the classified dataset for training and prediction, respectively. The 100 iterations were conducted to account for sites that may be more or less representative of a channel type and impact the prediction percentage. The average prediction rate of the 100 runs for the ANN and the GLM approaches were 79% and 77%, respectively, which are comparable results to the classification tree cross-validation percentage.

## Comparison of statistical reach-scale morphological classifications in the Sacramento River basin

Multivariate statistical analysis was used here to generate a data-driven classification for the particular basin geomorphology [kasprak\_blurred\_2016; sutfin\_geomorphic\_2014], which is in contrast to classifications based on preconceived definitions of reach-scale morphology. This approach is preferable when there is uncertainty as to what channel types exist in a region, and the larger the region the more likely there will be such uncertainty. On the other hand, it is possible that the larger the region, there might exist rare, unique channel types missed by sampling and thus not represented in a data-driven classification methodology. Further difficulty in multivariate statistical classification arises when selecting the appropriate number of final channel types. The classification is likely to make more physical sense with fewer channel types due to large differences in just a few channel attributes, but it may not be representative of the true geomorphic variability in a region of interest. However, uncorrelated channel attributes not influential in the highest statistical splits will likely be uniform across types as more dissimilar sites are lumped together. Alternatively, retaining more channel types may capture more variability across more attributes, but the multivariate nature of clustering may be capturing differences that have no physical meaning or conflicting physical meaning on various branches of a hierarchical clustering dendrogram. Statistical tests that help in selecting the number of stream classes (e.g. the NbClust package) were found to be more indicative of clustering based on valley confinement and sediment size, but less indicative of less statistically dominant differences in reach-scale morphology like TVAs, which are fundamental to hydraulic differences in forms and critical in many established channel classifications (e.g. plane bed vs. riffle-pool) [montgomery\_channel-reach\_1997].

The reach-scale morphological classification for the Sacramento River basin expands upon a previously developed data-driven sub-classification by lane\_role\_2017. lane\_role\_2017 only focused on sites in the LSR annual hydrological regime setting. The classification presented here includes 168 sites in other annual hydrological settings in addition to 120 in the LSR setting [lane\_role\_2017]. This classification also quantified and accounted for valley confinement as opposed to using it only for qualitative interpretation in the previous classification. Five outcomes can be observed in a qualitative reconciliation between the two classifications: comparable channel types, sub-channel

types exist in @lane\_role\_2017 compared to broader channel types in the present Sacramento basin classification, broader channel types exist in @lane\_role\_2017 compared to sub-channel types in the present Sacramento basin classification, channel types in the present classification do not exist in @lane\_role\_2017, and channel types in @lane\_role\_2017 do not exist in present Sacramento basin classification. More detailed relationships between the two classifications are presented in Table S4.

The Sacramento River basin reach-scale classification generally corresponds with other established classification systems. Here, we place our statistically-derived classification in the context of two of the most influential reach-scale classifications: The @montgomery\_channel-reach\_1997 classification of mountain systems and the Rosgen channel classification system [@rosgen\_classification\_1994; @rosgen\_applied\_1996]. A large majority of stream classes defined by @montgomery\_channel-reach\_1997 are represented here; however, a number of additional channel types and valley settings are represented in the Sacramento basin as well. It may be that in smaller and more homogeneous landscapes (e.g. all confined mountain streams) fewer channel types exist [@montgomery\_channel-reach\_1997]. The Sacramento basin classification indicates that valley confinement setting is likely to be important in differentiating channel types and associated hydrogeomorphic processes in more heterogeneous landscapes. Overly simplistic or insufficient channel types may miss key differences in form that may be important to physical interpretation or ecohydraulic conditions. The @rosgen\_applied\_1996 classification is more likely to encompass all channel types identified in the Sacramento Basin classification, but because it does not explicitly stratify channel types by valley confinement (which is not the same as Rosgen's entrenchment ratio), it misses an important landscape-scale topographic control on channel typology. Confinement plays an implicit role in the lettering in that system but is not alone at that level. @rosgen\_applied\_1996 has an independent qualitative valley classification system. The Rosgen classification is broad in nature to span many channel types, but is not quantitatively tested and proven, so our proposed statistical methodology is likely superior within a specific basin by characterizing distinct and regionally appropriate reach-scale morphologies and their continuum within a specific river basin. Given the binned sampling approach used here, the presented channel types represent both commonly observed and rare reach-scale morphologies specific to the Sacramento basin, but likely unsuitable for other regions.

Classification methods should be applicable in any region and support development of channel types that are physically interpretable, correspond with other established channel classifications, and incorporate regionally specific information to tailor classifications to the particularities of the region that may not be captured in more narrowly defined or broad classifications [@montgomery\_channel-reach\_1997; @rosgen\_applied\_1996]. This knowledge is key for fundamental understanding of regional river geomorphology and its interplay with hydrology. Furthermore, reach-scale classification provides a link to the defining physical habitat and ecohydraulics at locations within a river network [@kammel\_near-census\_2016; @lane\_integrated\_2018]. Therefore, it may support efforts to conserve and restore aquatic and riparian ecosystems that are key challenges in modern water resources management. For instance, reach scale classifications can be used to refine flow-ecology response relationships in well-established environmental flows methods such as ELOHA [@poff\_ecological\_2010].

Table S4. Comparison of reach-scale classification with Lane et al. (2017b).

Reconciliation Outcomes	Lane et al. (2017) channel types	Sacramento Basin channel types	Cause of reconciliation outcome
1. Comparable channel types	<ul style="list-style-type: none"> <li>* Confined headwater small boulder-cascade</li> <li>* Partly-confined large uniform</li> <li>* Unconfined large uniform boulder</li> </ul>	<ul style="list-style-type: none"> <li>* Confined boulder high-gradient step-pool/cascade</li> <li>* Partly-confined cobble-boulder uniform</li> <li>* Unconfined boulder-bedrock bed undulating</li> </ul>	<ul style="list-style-type: none"> <li>* Channel types that exist across both classifications are likely defined by distinct channel attributes and exist across a wide variety of landscapes</li> <li>* Differences in channel type naming strategies and final statistics that drive nomenclature result in different channel type names</li> </ul>
2. Sub-classifications in Lane et al. (2017) compared to broader channel types in present Sacramento basin classification	<ul style="list-style-type: none"> <li>* Unconfined upland plateau large uniform</li> <li>* Unconfined anastomosing plateau small pool-riffle</li> <li>* Partly-confined expansion pool-wide bar</li> </ul>	<ul style="list-style-type: none"> <li>* Unconfined low w/d gravel</li> <li>* Partly-confined high w/d gravel-cobble riffle-pool</li> </ul>	<ul style="list-style-type: none"> <li>* When combined with a larger number of sites across various landscape settings, unconfined plateau and partly-confined expansion sites do not statistically differentiate themselves from other unconfined and partly-confined sites, respectively</li> </ul>
3. Broader classifications in Lane et al. (2017) represented by multiple channel types in present Sacramento basin	<ul style="list-style-type: none"> <li>* Partly-confined pool-riffle</li> <li>* Confined cascade/step-pool</li> </ul>	<ul style="list-style-type: none"> <li>* Partly-confined high w/d gravel-cobble riffle-pool</li> <li>* Partly-confined low w/d gravel-cobble riffle-pool</li> <li>* Confined boulder-bedrock low-gradient step-pool</li> <li>* Confined boulder-bedrock uniform</li> </ul>	<ul style="list-style-type: none"> <li>* Differences in w/d proved significant to define two types of riffle-pool streams in partly-confined settings, while variability metrics differentiated between step-pool and uniform streams of similar slope</li> </ul>
4. Channel types in the present classification do not exist in Lane et al. (2017)	—	<ul style="list-style-type: none"> <li>* Confined gravel-cobble uniform</li> <li>* Unconfined gravel-cobble riffle-pool</li> </ul>	<ul style="list-style-type: none"> <li>* Channel types exist in current classification, but not in Lane et al. (2017) due to the addition of sites in other landscape settings</li> </ul>
5. Channel types in Lane et al. (2017) do not exist in present Sacramento basin classification	<ul style="list-style-type: none"> <li>* Unconfined large meandering sand bed</li> </ul>	—	<ul style="list-style-type: none"> <li>* Changes in the defining hydrological settings of certain sites was changed between morphological classifications leading to those sites being excluded from the present classification (Lane et al., 2018)</li> </ul>

## Site data

Table S5. Reach-scale data for all sites used in geomorphic classification.

	Ac	s	d	w	w/d	d/D50	CVd	CVw	k	D50	D84	Cv	Ls
HLP_518KNCAWC	47	0.041	0.5	13.0	25.8	2.0	0.12	0.42	1.1	248	1000	108	150
HLP_526CE0323	157	0.029	1.3	7.7	6.1	260.0	0.12	0.44	1.1	5	95	262	150
HLP_526PS0072	361	0.016	0.7	5.6	7.7	8.2	0.16	0.14	1.2	85	757	34	750
HLP_526PS0396	71	0.022	0.3	1.9	5.6	6.7	0.37	0.32	1.4	45	1000	2501	144
HLP_526PS0440	275	0.020	0.7	4.8	7.3	10.8	0.11	0.33	1.2	65	270	821	150
HLP_526PS1420	76	0.028	0.4	1.3	3.1	20.0	0.19	0.54	1.2	20	193	32	150
HLP_526PSCBBL	35	0.047	0.5	2.8	6.2	9.6	0.18	0.17	1.1	52	1000	0	150
HLP_526PSCBLK	14	0.005	0.4	3.3	7.8	200.0	0.08	0.22	1.3	2	2	1155	150
HLP_526WE0506	275	0.024	0.4	13.7	32.7	1.6	0.43	0.44	1.2	250	2500	172	150
HLP_526WTCACT	88	0.042	1.3	4.4	3.3	9.4	0.21	0.32	1.4	138	3400	9	150
HLP_527CE0093	13	0.054	0.4	2.7	6.5	25.0	0.32	0.36	1.3	16	250	36	298
HLP_527PS0388	32	0.015	0.5	1.8	3.8	17.2	0.18	0.21	1.1	29	77	65	143
HLP_527PS1156	18	0.042	0.5	2.1	4.4	13.9	0.20	0.27	1.1	36	111	26	150
HLP_527PS1412	25	0.043	0.6	2.4	4.0	22.2	0.17	0.16	1.3	27	147	72	150
HLP_527SED084	44	0.007	0.3	4.3	17.2	30.0	0.28	0.23	1.1	10	40	1682	293
HLP_3	45	0.010	0.3	8.8	33.7	0.1	0.21	0.03	1.7	3	6	3320	150
HLP_4	1030	0.020	1.3	10.5	12.9	0.1	0.05	0.22	1.1	11	190	5000	150
HLP_10	71	0.039	1.2	10.6	8.6	6.3	0.25	0.24	1.2	190	5000	616	150
HLP_24	44	0.007	0.4	16.0	37.3	0.4	0.11	0.26	1.3	1000	5000	536	150
HLP_28	233	0.003	0.5	23.1	47.1	2.6	0.28	0.43	1.2	190	5000	5000	150
HLP_37	591	0.012	0.9	8.2	8.9	4.7	0.12	0.29	1.4	190	5000	2628	150
HLP_53	7498	0.006	0.9	16.8	19.1	0.9	0.46	0.20	1.1	1000	5000	2509	150
HLP_54	7498	0.005	0.9	18.9	21.8	0.9	0.41	0.23	1.3	1000	5000	1956	250
HLP_55	7434	0.004	1.1	15.2	14.5	8.2	0.58	0.21	1.1	128	5000	449	150
HLP_59	7398	0.001	0.8	7.4	9.9	8.3	0.52	0.31	1.1	90	5000	404	150
LSR_504PS0227	544	0.009	1.6	30.7	19.1	16.0	0.25	0.31	1.3	100	250	4728	250
LSR_505BMC MCR	4	0.098	0.7	7.3	10.0	2.6	0.20	0.35	1.2	280	820	44	150
LSR_505CE0137	31	0.032	1.1	3.7	3.7	66.0	0.23	0.35	1.1	16	250	3150	148
LSR_505LBCAMR	9	0.143	0.9	7.1	8.7	2.2	0.22	0.28	1.2	390	2500	25	150
LSR_505PS0156	624	0.018	1.5	15.7	10.9	27.1	0.10	0.14	1.8	54	1000	0	250
LSR_505PS1180	187	0.023	1.1	14.1	16.3	15.1	0.53	0.27	1.7	75	205	2119	300
LSR_507CE0581	84	0.048	0.7	9.1	14.4	2.7	0.19	0.28	1.2	250	2500	14	198
LSR_507MZCAML	20	0.075	1.0	6.4	6.9	24.8	0.19	0.27	1.2	39	165	34	150
LSR_507PS0122	366	0.017	1.3	11.4	12.6	25.6	0.25	0.26	1.2	50	2500	108	150
LSR_507PS0286	6	0.076	0.4	2.3	5.8	5.6	0.26	0.42	1.1	79	2500	272	134
LSR_507PS0314	488	0.020	2.0	10.9	5.7	8.0	0.22	0.13	1.3	250	2500	28	150
LSR_507SHA915	68	0.048	1.1	9.5	8.7	17.2	0.29	0.17	1.4	64	5000	226	150
LSR_507WE0988	21	0.028	0.4	6.8	19.8	1.4	0.23	0.24	1.2	250	1000	1707	150
LSR_509ACNFPP	108	0.027	1.3	12.7	10.0	12.2	0.26	0.15	1.1	110	1000	114	600
LSR_509ACSFPP	119	0.028	1.5	16.6	11.2	18.6	0.18	0.44	1.2	80	1000	112	150
LSR_509ATCINC	231	0.017	1.2	16.2	13.4	14.0	0.11	0.06	1.3	87	1000	129	150
LSR_509BCCH32	48	0.026	1.3	11.7	9.4	10.1	0.18	0.20	1.1	130	1000	34	150
LSR_509BSCADC	22	0.048	0.7	6.7	10.0	3.5	0.17	0.19	1.2	200	1000	9	150
LSR_509CBCADC	16	0.079	1.3	7.4	6.1	1.3	0.20	0.22	1.5	1000	5000	30	150
LSR_509CTCADC	5	0.016	0.5	4.4	8.4	255.5	0.22	0.52	1.5	2	20	17	150

Table S5 (cont'd). Reach-scale data for all sites used in geomorphic classification (cont'd).

	Ac	s	d	w	w/d	d/D50	CVd	CVw	k	D50	D84	Cv	Ls
LSR_509DCPWxx	439	0.021	1.5	22.3	18.5	1.5	0.69	0.25	1.3	1000	2500	35	250
LSR_509DRCBPC	316	0.028	1.2	21.5	19.1	3.9	0.15	0.19	1.2	300	1000	130	250
LSR_509ICPPCX	261	0.044	1.0	8.3	9.7	12.0	0.20	0.25	1.3	79	1000	118	300
LSR_509PS0049	79	0.015	1.2	39.0	34.5	579.1	0.31	0.47	1.5	2	64	437	285
LSR_509PS0085	132	0.042	1.8	20.6	12.6	7.1	0.22	0.26	1.3	250	2500	12	240
LSR_509PS0170	22	0.034	0.8	7.4	9.8	15.5	0.16	0.23	1.1	50	350	34	150
LSR_509PS0234	261	0.016	1.1	15.5	15.1	5.2	0.27	0.11	1.3	210	1000	56	500
LSR_514DNCLDC	24	0.036	1.0	9.7	10.9	1.0	0.21	0.23	1.2	1000	5000	10	150
LSR_514PS0099	500	0.015	2.1	25.6	13.7	5.6	0.35	0.23	1.2	370	5000	28	250
LSR_514SED078	76	0.011	0.7	20.8	28.9	11.3	0.19	0.15	1.3	64	250	1124	250
LSR_517LCCAYB	12	0.022	0.4	4.3	12.7	5.6	0.39	0.38	1.2	75	190	333	143
LSR_517PS0054	56	0.047	1.8	14.6	9.3	1.2	0.29	0.30	1.4	2500	5000	42	150
LSR_517PS0061	18	0.053	1.7	9.9	6.9	6.8	0.35	0.42	1.3	250	5000	105	150
LSR_517PS0074	25	0.042	1.1	12.2	11.1	6.3	0.19	0.20	1.2	180	1000	101	150
LSR_517WE0515	375	0.007	0.8	13.4	18.8	3.1	0.22	0.33	1.3	250	5000	15	150
LSR_518BTCASC	53	0.025	0.7	10.7	14.7	8.3	0.21	0.14	1.1	90	315	323	150
LSR_518CE0015	460	0.013	0.9	20.0	23.7	3.5	0.24	0.14	1.3	250	1000	36	425
LSR_518CE0034	64	0.020	0.9	14.4	17.1	3.6	0.24	0.17	1.4	250	1000	53	277
LSR_518CE0047	34	0.025	0.3	10.6	42.5	4.0	0.22	0.29	1.2	64	250	3140	148
LSR_518CE0114	1633	0.052	1.1	14.3	14.7	4.2	0.21	0.27	1.4	250	2500	26	376
LSR_518CE0242	26	0.015	0.5	9.8	19.9	7.8	0.10	0.04	1.4	64	64	1008	148
LSR_518CE0338	4	0.106	1.2	9.3	8.3	15.9	0.12	0.36	1.1	72	1000	81	150
LSR_518CE0543	238	0.005	0.5	12.3	26.6	230.0	0.21	0.21	1.1	2	2	3455	148
LSR_518CE0575	21	0.006	0.5	3.0	5.9	270.0	0.19	0.42	1.3	2	16	3302	141
LSR_518CE0879	1911	0.008	1.5	20.0	14.9	725.0	0.29	0.26	1.2	2	16	1160	198
LSR_518CE0895	2	0.013	1.0	8.5	8.3	64.6	0.24	0.24	1.5	16	64	3993	148
LSR_518CPCRCR	46	0.044	2.2	13.5	6.5	18.7	0.34	0.19	1.4	120	2500	38	300
LSR_518GZCUPx	35	0.013	1.0	13.1	15.3	13.5	0.35	0.25	1.4	71	1000	110	450
LSR_518PS0017	61	0.015	0.9	16.1	20.4	7.4	0.39	0.14	1.3	120	5000	12	150
LSR_518PS0029	526	0.040	1.2	12.4	11.0	3.7	0.29	0.37	1.2	320	2500	38	300
LSR_518PS0033	5	0.091	0.7	6.6	9.4	9.7	0.20	0.26	1.2	74	5000	12	143
LSR_518PS0045	11	0.052	0.5	5.5	12.4	1.7	0.29	0.49	1.3	280	5000	0	135
LSR_518PS0089	29	0.005	0.3	6.2	18.8	170.0	0.15	0.32	1.1	2	2	563	285
LSR_518PS0093	70	0.049	0.6	10.3	17.6	8.3	0.20	0.13	1.3	74	430	68	150
LSR_518PS0113	34	0.049	1.1	11.6	10.6	9.0	0.20	0.26	1.1	126	1000	22	150
LSR_518PS0125	1872	0.013	1.5	19.8	13.1	22.1	0.16	0.30	1.3	69	1000	12	250
LSR_518RCNAPC	27	0.024	1.2	17.2	14.9	16.2	0.22	0.28	1.3	75	270	1794	150
LSR_518SDCAHR	65	0.011	0.7	4.9	6.6	30.6	0.20	0.37	1.4	24	69	1005	150
LSR_518SED013	53	0.012	0.7	9.5	14.6	11.2	0.21	0.43	1.3	58	250	603	150
LSR_518SED015	60	0.005	0.6	13.6	21.2	33.7	0.20	0.21	1.1	19	73	397	250
LSR_518SED082	20	0.004	0.8	13.1	17.5	107.1	0.60	0.21	1.1	7	64	172	150
LSR_518SED086	50	0.032	1.0	10.8	11.6	10.5	0.29	0.17	1.4	95	2500	10	300
LSR_518SED089	30	0.011	0.2	6.0	31.7	4.9	0.29	0.09	2.0	40	150	430	150
LSR_518SED091	38	0.011	0.5	8.8	17.9	30.6	0.51	0.28	1.1	16	64	1008	150
LSR_518SNABC	52	0.028	0.5	4.0	7.8	17.4	0.18	0.30	1.1	30	97	185	143

Table S5 (cont'd). Reach-scale data for all sites used in geomorphic classification (cont'd).

	Ac	s	d	w	w/d	d/D50	CVd	CVw	k	D50	D84	Cv	Ls
LSR_518WE0521	60	0.020	1.4	14.9	10.9	15.9	0.17	0.23	1.3	88	310	61	150
LSR_518WLCBCP	24	0.031	0.4	1.6	4.0	30.9	0.24	0.39	1.2	13	49	1294	128
LSR_518WLCBWL	20	0.036	0.7	25.0	37.2	38.0	0.14	0.00	1.1	18	91	281	143
LSR_518YLCAFR	199	0.030	1.9	16.8	10.5	6.6	0.44	0.22	1.7	290	5000	0	250
LSR_521BTCLBC	305	0.014	0.9	8.5	9.2	470.5	0.14	0.08	1.2	2	5000	270	250
LSR_522GSCBSC	262	0.018	0.6	11.5	22.0	11.8	0.36	0.26	1.3	50	120	28	150
LSR_522MFSCRB	83	0.021	0.8	9.1	11.8	18.1	0.21	0.15	1.4	45	1000	21	150
LSR_522PS0430	247	0.030	1.1	14.5	13.9	11.7	0.18	0.13	1.4	93	1000	12	250
LSR_522WE0767	36	0.015	0.4	7.4	20.6	6.1	0.21	0.36	1.3	64	5000	21	150
LSR_523PS0172	9	0.075	1.0	5.3	5.3	9.2	0.09	0.24	1.2	110	2500	6	150
LSR_523PS0414	67	0.041	1.2	9.3	8.7	18.5	0.22	0.22	1.3	64	5000	6	150
LSR_523TMCATG	409	0.041	0.7	15.5	23.9	5.7	0.12	0.15	1.3	115	2500	8	150
LSR_523WE0512	67	0.029	0.4	6.8	20.7	5.4	0.20	0.21	1.4	64	2500	0	150
LSR_526CE0341	90	0.050	0.8	11.8	17.5	0.8	0.31	0.22	1.2	1000	2500	12	200
LSR_526CE0483	9	0.070	0.5	4.7	11.3	7.8	0.25	0.28	1.3	57	520	774	298
LSR_526PS0220	469	0.019	1.3	18.6	14.3	1.3	0.18	0.14	2.2	1000	1000	491	250
LSR_526PS0356	767	0.001	1.3	8.1	6.4	655.0	0.22	0.49	1.4	2	26	4820	150
LSR_526WE0744	154	0.026	0.4	11.2	31.6	0.2	0.14	0.26	1.2	2500	2500	31	150
LSR_0	298	0.002	0.7	18.4	25.2	11.4	0.27	0.14	1.1	64	90	3331	250
LSR_1	15	0.003	1.4	10.0	7.3	85.1	0.33	0.39	1.1	16	32	477	150
LSR_2	86	0.005	0.8	10.1	13.1	17.1	0.23	0.18	1.1	45	90	1174	150
LSR_5	101	0.050	0.8	6.6	8.5	17.2	0.18	0.20	1.3	45	90	3566	250
LSR_6	46	0.011	0.5	5.1	9.8	185.1	0.38	0.31	1.1	3	45	4386	150
LSR_7	1299	0.011	0.8	14.9	18.1	0.8	0.34	0.15	1.2	1000	5000	8	250
LSR_8	4	0.024	0.4	6.5	15.6	6.5	0.18	0.31	1.1	64	190	294	250
LSR_9	221	0.006	0.6	7.2	12.7	6.3	0.22	0.17	1.0	90	5000	5000	150
LSR_11	78	0.031	0.5	6.6	14.2	0.5	0.50	0.27	1.1	1000	5000	3606	150
LSR_12	4	0.026	0.9	3.5	3.9	7.0	0.24	0.27	1.1	128	5000	67	250
LSR_13	21	0.008	0.3	5.3	16.5	2.5	0.18	0.23	1.0	128	5000	78	150
LSR_14	148	0.033	1.8	14.8	8.1	1.8	0.12	0.51	1.3	1000	5000	10	250
LSR_15	11	0.033	0.6	5.9	10.4	12.5	0.29	0.24	1.2	45	5000	74	150
LSR_16	14	0.008	0.6	4.8	8.7	6.2	0.41	0.37	1.1	90	5000	80	150
LSR_17	33	0.016	0.9	6.4	6.8	0.9	0.21	0.62	1.1	1000	5000	214	150
LSR_18	181	0.008	1.0	16.0	15.4	8.1	0.60	0.25	1.1	128	5000	42	250
LSR_20	6	0.015	0.6	4.3	6.9	6.3	0.61	0.35	1.1	90	5000	10	150
LSR_21	8	0.024	0.4	2.3	6.4	4.0	0.64	0.29	1.1	90	5000	77	150
LSR_22	36	0.033	0.7	7.7	11.0	7.8	0.25	0.33	1.2	90	5000	190	250
LSR_23	13	0.026	1.3	7.7	5.9	1.3	0.18	0.20	1.1	1000	5000	4	150
LSR_25	733	0.016	0.8	2.3	2.9	0.8	0.46	0.14	1.2	1000	5000	4564	250
LSR_29	52	0.008	0.6	5.8	9.9	6.5	0.32	0.20	1.0	90	5000	203	150
LSR_32	821	0.010	1.9	33.4	17.5	1.9	0.23	0.21	1.1	1000	5000	82	250
LSR_34	1872	0.001	1.2	16.9	14.1	18.7	0.26	0.20	1.2	64	5000	33	250
LSR_36	250	0.006	0.7	14.0	20.3	10.8	0.40	0.35	1.4	64	190	17	250
LSR_38	288	0.017	0.7	9.2	13.4	10.2	0.35	0.43	1.1	90	190	34	250
LSR_40	123	0.015	1.5	17.3	11.4	1.5	0.21	0.24	1.1	1000	5000	142	150



Table S5 (cont'd). Reach-scale data for all sites used in geomorphic classification (cont'd).

	Ac	s	d	w	w/d	d/D50	CVd	CVw	k	D50	D84	Cv	Ls
LSR_41	417	0.0090	1.4	26.1	18.8	7.3	0.23	0.09	1.1	190	5000	68	250
LSR_42	723	0.0030	1.2	33.5	28.5	26.1	0.19	0.06	1.1	45	128	197	250
LSR_43	182	0.0040	0.7	6.3	8.6	11.5	0.38	0.41	1.4	64	5000	10	150
LSR_44	98	0.0280	0.8	11.7	15.1	4.1	0.15	0.10	1.0	190	2500	110	150
LSR_45	821	0.0010	1.5	24.1	15.7	12.0	0.41	0.22	1.2	128	5000	0	250
LSR_46	196	0.0090	0.7	13.1	18.5	7.9	0.24	0.20	1.2	90	5000	110	250
LSR_47	633	0.0080	1.1	19.1	17.1	1.1	0.21	0.31	1.2	1000	5000	36	250
LSR_48	312	0.0010	0.6	10.6	18.5	35.7	0.29	0.25	1.3	16	32	8	250
LSR_49	371	0.0300	0.6	18.2	30.5	0.6	0.36	0.52	1.2	1000	5000	9	250
LSR_50	47	0.0180	0.7	7.2	10.6	5.3	0.25	0.16	1.1	128	5000	251	150
PGR_0	14	0.0006	0.7	4.8	6.7	89.6	0.45	0.16	1.1	8	23	1106	150
PGR_2	221	0.0001	1.5	10.7	7.3	132.5	0.11	0.17	1.1	11	23	178	150
PGR_3	90	0.0040	2.1	47.0	22.9	64.0	0.21	0.57	1.1	32	64	687	250
PGR_4	47	0.0065	0.7	10.3	14.4	44.8	0.41	0.18	1.2	16	64	53	150
PGR_5	32	0.0107	0.7	6.1	9.2	10.4	0.30	0.34	1.2	64	90	1452	150
PGR_6	246	0.0041	1.5	18.4	12.7	11.4	0.19	0.20	1.2	128	200	117	250
PGR_7	48	0.0118	0.8	10.9	13.4	51.0	0.26	0.16	1.1	16	128	28	150
PGR_8	168	0.0150	2.8	13.9	5.0	0.7	0.23	0.19	1.1	5000	5000	2	150
PGR_9	48	0.0090	0.7	9.7	13.6	64.5	0.24	0.13	1.2	11	90	15	150
PGR_10	67	0.0043	0.8	9.5	11.7	101.8	0.58	0.20	1.5	8	64	91	150
PGR_11	19	0.0126	0.7	8.4	11.9	15.6	0.19	0.27	1.1	45	128	55	150
PGR_12	32	0.0109	0.7	5.2	7.5	10.7	0.14	0.18	1.1	64	190	2	150
PGR_13	6	0.0023	1.1	4.6	4.1	12.4	0.26	0.42	1.1	90	5000	1	150
PGR_14	101	0.0088	1.6	14.6	9.5	24.2	0.25	0.19	1.3	64	1000	23	150
PGR_15	6	0.0153	0.7	5.3	7.3	0.2	0.20	0.42	1.2	5000	5000	0	150
PGR_16	245	0.0206	0.6	7.1	11.0	10.1	0.27	0.27	1.1	64	200	31	150
PGR_17	164	0.0051	1.0	15.3	15.3	91.3	0.25	0.18	1.2	11	23	217	150
PGR_18	10	0.0027	1.5	6.9	4.7	1.5	0.20	0.23	1.2	1000	5000	5	150
PGR_19	398	0.0002	1.1	14.5	13.1	12.3	0.26	0.17	1.5	90	190	10	250
PGR_20	52	0.0107	1.4	12.9	9.2	31.2	0.15	0.13	1.6	45	1000	104	150
PGR_21	16	0.0005	1.3	10.4	7.7	7.1	0.27	0.13	1.2	190	1000	21	150
PGR_22	38	0.0053	0.8	10.4	13.1	24.7	0.27	0.22	1.1	32	128	4	150
PGR_23	8	0.0007	0.8	6.3	7.6	51.5	0.15	0.13	1.3	16	32	790	150
PGR_24	5	0.0058	0.4	3.3	9.3	11.2	0.37	0.49	1.2	32	64	361	150
PGR_25	971	0.0011	0.9	23.0	25.9	27.7	0.43	0.53	1.1	32	64	1260	150
PGR_26	220	0.0011	1.5	15.0	10.2	261.4	0.21	0.19	1.1	6	11	118	150
PGR_27	6	0.0050	0.7	4.4	6.5	15.2	0.12	0.37	1.1	45	200	9	150
PGR_28	1025	0.0091	1.1	20.9	19.1	24.3	0.37	0.29	1.2	45	90	2671	250
PGR_29	43	0.0084	1.3	10.3	8.1	637.3	0.30	0.38	1.8	2	45	1280	150
PGR_30	34	0.0003	0.5	2.6	5.4	240.5	0.17	0.24	1.2	2	8	4986	150
PGR_31	317	0.0185	0.9	6.5	7.3	19.8	0.34	0.44	1.3	45	5000	12	150
PGR_32	5	0.0014	0.9	6.1	6.7	14.1	0.38	0.19	1.1	64	200	303	150
PGR_33	17	0.0140	0.9	7.0	7.5	234.6	0.43	0.28	1.2	4	32	96	150
PGR_34	23	0.0039	1.1	23.6	21.4	49.0	0.28	0.25	1.1	23	64	1955	250
PGR_35	19	0.0033	0.7	5.6	8.6	40.5	0.34	0.43	1.3	16	45	1201	150

Table S5 (cont'd). Reach-scale data for all sites used in geomorphic classification (cont'd).

	Ac	s	d	w	w/d	d/D50	CVd	CVw	k	D50	D84	Cv	Ls
PGR_36	11	0.0048	1.2	9.2	7.7	74.1	0.34	0.33	1.1	16	90	92	150
PGR_37	21	0.0054	1.4	7.7	5.6	7.3	0.21	0.21	1.2	190	5000	23	150
PGR_38	3	0.0308	0.6	4.0	6.7	4.7	0.60	0.25	1.1	128	1000	12	150
PGR_41	46	0.0143	0.9	6.6	7.4	4.7	0.22	0.18	1.3	190	5000	41	150
PGR_42	42	0.0025	0.8	7.3	9.4	17.3	0.31	0.35	1.4	45	200	3	150
PGR_43	48	0.0057	0.9	11.7	12.7	10.2	0.35	0.29	1.2	90	200	69	150
PGR_44	135	0.0013	1.1	15.5	14.1	68.8	0.30	0.26	1.1	16	32	1647	150
PGR_45	204	0.0014	1.0	9.1	9.1	250.5	0.57	0.17	1.1	4	11	1710	150
PGR_47	1027	0.0092	1.0	28.0	28.0	62.4	0.44	0.21	1.1	16	45	3193	250
PGR_509BCCBPW	164	0.0142	0.7	16.9	23.6	5.8	0.27	0.07	1.3	125	1000	155	250
PGR_513PS0024	26	0.0280	3.2	14.2	4.4	50.4	0.30	0.19	1.2	64	5000	11	250
PGR_504CE0210	193	0.0155	1.6	15.1	10.0	6.4	0.26	0.16	1.1	250	250	4771	250
PGR_508PS0458	614	0.0240	0.8	26.6	34.1	27.3	0.19	0.11	1.0	30	79	527	250
PGR_513PS0088	577	0.0185	0.9	10.2	12.1	23.1	0.20	0.32	1.1	40	95	97	250
PGR_513PS0200	96	0.0155	0.8	9.0	12.3	22.1	0.31	0.19	1.3	37	115	76	150
PGR_524PS0202	299	0.0070	1.1	20.4	20.8	26.1	0.34	0.21	1.1	41	140	166	250
PGR_513PS0248	62	0.0200	0.6	7.8	15.1	7.9	0.26	0.10	1.1	70	240	24	150
PGR_524SHA916	271	0.0150	1.7	12.5	7.5	16.5	0.27	0.17	1.2	80	5000	73	250
PGR_513BTCACC	46	0.0260	0.5	5.5	12.4	5.0	0.34	0.26	1.2	100	5000	17	150
RGW_0	8	0.0260	0.9	5.8	6.9	0.9	0.39	0.30	1.3	1000	5000	3	150
RGW_1	6	0.0230	0.4	5.3	13.8	12.1	0.51	0.28	1.1	32	200	1	150
RGW_2	37	0.0060	0.8	8.8	11.3	6.1	0.32	0.10	1.1	128	200	62	150
RGW_3	40	0.0090	1.1	18.1	16.2	5.9	0.14	0.21	1.4	190	5000	95	250
RGW_4	241	0.0030	1.8	36.1	19.6	115.0	0.63	0.19	1.1	16	45	1707	250
RGW_5	5	0.0110	0.4	3.4	8.1	9.2	0.20	0.22	1.1	45	90	235	150
RGW_6	35	0.0035	0.4	7.4	19.6	34.5	0.42	0.23	1.2	11	16	748	150
RGW_7	5	0.0060	1.2	15.1	12.4	1.2	0.78	0.32	1.3	1000	1000	233	150
RGW_8	197	0.0030	1.3	13.2	10.5	39.2	0.19	0.22	1.2	32	64	5000	250
RGW_9	263	0.0020	2.1	22.0	10.7	16.1	0.24	0.44	1.2	128	5000	4	250
RGW_10	22	0.0090	0.8	11.2	14.3	0.8	0.28	0.31	1.3	1000	1000	221	150
RGW_11	52	0.0060	1.1	14.6	13.8	66.2	0.27	0.51	1.1	16	64	63	150
RGW_12	7	0.0080	0.5	3.1	6.7	14.5	0.18	0.16	1.0	32	128	9	150
RGW_15	97	0.0080	0.8	9.4	12.3	47.7	0.20	0.15	1.1	16	32	4889	150
RGW_16	97	0.0010	1.3	12.2	9.2	29.5	0.21	0.25	1.1	45	200	812	150
RGW_18	41	0.0370	1.4	9.9	7.1	0.4	0.34	0.32	1.3	5000	5000	0	150
RGW_23	79	0.0030	0.8	6.7	8.8	8.4	0.42	0.25	1.3	90	5000	817	150
RGW_27	10	0.0030	0.7	4.6	6.4	129.7	0.17	0.15	1.3	6	16	1365	150
RGW_29	195	0.0020	1.0	11.6	11.5	5.3	0.31	0.10	1.2	190	5000	18	150
RGW_31	181	0.0010	1.0	16.1	15.6	128.9	0.24	0.10	1.3	8	32	5000	250
RGW_36	327	0.0040	0.9	15.1	17.5	13.4	0.23	0.25	1.1	64	128	4269	250
RGW_37	136	0.0040	1.3	9.9	7.6	118.8	0.23	0.20	1.4	11	23	1124	150
RGW_41	43	0.0200	1.4	8.7	6.3	6.9	0.21	0.21	1.0	200	5000	233	150
RGW_42	40	0.0020	1.0	9.4	9.5	15.5	0.30	0.15	1.3	64	200	93	250
RGW_43	31	0.0200	1.0	11.7	11.6	5.3	0.32	0.16	1.1	190	5000	29	150
RGW_44	7	0.0130	1.1	7.2	6.7	0.3	0.35	0.35	1.6	5000	5000	53	150

Table S5 (cont'd). Reach-scale data for all sites used in geomorphic classification (cont'd).

	Ac	s	d	w	w/d	d/D50	CVd	CVw	k	D50	D84	Cv	Ls
RGW_45	4	0.0200	0.5	6.8	12.6	6.0	0.31	0.39	1.2	90	1000	41	150
RGW_46	9	0.0270	0.7	6.6	9.4	15.5	0.10	0.18	1.0	45	128	17	150
RGW_47	40	0.0070	1.2	12.4	10.4	13.2	0.18	0.29	1.1	90	200	1488	250
RGW_48	4	0.0060	0.6	5.5	8.9	0.6	0.16	0.19	1.1	1000	1000	5	150
RGW_50	8	0.0080	0.8	16.3	20.0	4.1	0.27	0.22	1.2	200	1000	9	250
RGW_51	52	0.0100	1.3	11.0	8.9	6.2	0.40	0.31	1.1	200	5000	1415	150
RGW_507CE0181	27	0.0200	0.6	4.1	7.6	2.2	0.21	0.24	1.1	250	1000	764	150
RGW_520CE0562	87	0.0110	1.4	11.0	8.2	21.2	0.11	0.04	1.2	64	250	4808	250
RGW_509PCDTWR	21	0.0250	1.1	7.2	6.6	17.4	0.16	0.11	1.0	64	115	72	150
RGW_514CE0139	39	0.0270	0.6	8.2	15.4	2.2	0.36	0.40	1.2	250	1000	598	150
RGW_514PS0351	37	0.0150	1.3	17.1	13.3	10.9	0.09	0.18	1.1	120	380	313	250
RGW_513PS0008	19	0.0290	1.2	9.1	8.6	14.7	0.37	0.29	1.2	80	1000	0	150
RGW_513STCAIV	8	0.0480	1.0	7.7	8.1	5.8	0.14	0.43	1.1	150	450	36	150
RGW_517PS0078	19	0.0350	0.7	5.8	9.0	7.3	0.21	0.32	1.2	92	1000	448	150
RGW_514CE0555	63	0.0580	0.3	2.7	8.2	1.3	0.24	0.27	1.2	250	1000	2	150
RGW_504PS0019	199	0.0060	0.8	7.9	10.2	35.1	0.32	0.13	1.1	22	40	4688	150
RGW_504CE0657	1	0.0110	0.5	6.1	16.4	7.1	0.59	0.37	1.4	64	250	5000	150
RGW_504PS0051	74	0.0210	1.3	22.2	17.1	23.9	0.13	0.30	1.2	55	185	4579	250
RGW_504PS0371	161	0.0100	1.0	14.6	18.2	40.6	0.58	0.28	1.1	24	80	4499	250
RGW_507PS0142	196	0.0130	1.5	21.2	16.3	17.2	0.24	0.41	1.3	85	250	295	250
RGW_508BERPRK	292	0.0110	1.4	12.4	10.0	22.2	0.38	0.26	1.0	95	5000	468	250
RGW_504DCFRxx	69	0.0360	1.5	8.1	6.0	5.9	0.49	0.34	1.1	250	5000	23	150
RGW_504WE0527	68	0.0290	1.7	17.8	10.4	7.2	0.09	0.10	1.1	250	2500	24	250
RGW_509CE0305	285	0.0210	1.0	19.6	22.3	15.8	0.48	0.31	1.2	80	192	98	250
RGW_509PS0334	302	0.0190	1.8	18.6	10.6	19.8	0.15	0.30	1.1	90	380	94	250
WS_0	77	0.0040	0.6	6.0	10.0	6.6	0.03	0.01	1.8	90	5000	19	250
WS_1	93	0.0030	0.8	7.4	9.4	280.5	0.24	0.18	1.1	3	23	65	150
WS_3	33	0.0290	0.2	3.2	14.5	7.0	0.04	0.02	1.1	32	128	670	250
WS_4	100	0.0010	1.1	11.1	10.1	69.2	0.12	0.32	1.4	16	45	731	250
WS_5	69	0.0030	0.5	8.0	16.1	89.3	0.45	0.20	1.5	6	32	401	150
WS_7	57	0.0030	1.0	12.0	11.6	8.1	0.16	0.11	1.1	128	200	27	150
WS_9	10	0.0170	0.6	4.2	6.9	4.8	0.33	0.28	1.1	128	5000	23	150
WS_10	69	0.0038	0.7	12.1	18.1	29.7	0.28	0.11	1.3	23	45	466	150
WS_11	32	0.0140	1.1	8.1	7.5	5.4	0.23	0.10	1.1	200	5000	5	150
WS_12	25	0.0090	0.9	7.4	8.8	9.4	0.23	0.15	1.1	90	200	56	150
WS_13	100	0.0040	1.0	8.3	8.2	62.8	0.29	0.12	1.3	16	45	580	150
WS_14	83	0.0160	0.8	13.2	15.6	37.3	0.27	0.26	1.3	23	200	64	150
WS_16	6	0.0170	0.7	4.4	3.6	7.3	0.28	0.25	1.3	90	1000	2	150
WS_17	10	0.0050	0.4	5.4	13.2	72.9	0.32	0.30	1.4	6	64	144	150
WS_18	6	0.0140	0.6	4.3	7.4	104.2	0.22	0.23	1.1	6	23	866	150
WS_20	69	0.0000	1.2	7.1	6.0	588.6	0.22	0.22	1.1	2	2	4375	150
WS_514PS0084	7	0.0000	0.5	4.0	7.9	51.0	0.41	0.78	1.1	10	1000	3842	150
WS_515PS0490	30	0.0010	1.0	6.7	6.7	515.0	0.20	0.06	1.1	2	2	4688	150
WS_520PS0202	25	0.0010	1.0	8.4	8.7	480.0	0.23	0.29	1.2	2	2	5000	150
WS_511CE0663	35	0.0120	1.6	7.6	4.9	815.0	0.23	0.13	1.2	2	250	1922	150

Table S5 (cont'd). Reach-scale data for all sites used in geomorphic classification (cont'd).

	Ac	s	d	w	w/d	d/D50	CVd	CVw	k	D50	D84	Cv	Ls
WS_514CE0523	7	0.012	0.7	4.3	7.6	325.0	0.29	0.21	1.2	2	16	297	150
WS_519CE0019	22	0.007	0.7	4.3	6.6	340.0	0.26	0.11	1.3	2	2	5000	150
WS_519CE0363	9	0.014	1.0	5.1	5.1	70.0	0.22	0.27	1.4	14	27	1197	150
WS_519CE0531	7	0.006	1.0	2.7	3.2	500.0	0.74	0.33	1.7	2	2	4375	150
WS_505PS0110	31	0.029	1.2	7.8	7.1	1.2	0.40	0.21	1.2	1000	5000	18	150
WS_506PS0003	16	0.030	1.0	5.8	7.7	4.2	0.70	0.32	1.2	245	5000	28	150
WS_506PS0062	11	0.047	0.6	5.1	8.8	7.5	0.15	0.18	1.1	80	350	15	150
WS_524SHA907	14	0.055	2.7	11.5	4.9	53.0	0.42	0.45	1.2	50	5000	11	250
WS_521LCCBSR	6	0.050	0.5	7.0	13.5	7.2	0.12	0.16	1.0	74	1000	17	150
WS_508SHA910	84	0.015	0.9	22.1	23.8	21.6	0.16	0.28	1.6	43	110	3066	250
WS_508SHA911	89	0.010	2.3	17.3	11.1	97.5	0.76	0.43	1.1	24	55	3279	250
WS_508SHA912	153	0.010	1.6	17.0	13.4	42.6	0.49	0.18	1.1	38	72	3777	250
WS_511PS0401	55	0.030	2.6	8.8	3.4	1285.0	0.07	0.15	1.2	2	13	4175	150
WS_514CE0171	56	0.016	1.8	14.3	8.2	28.0	0.15	0.15	1.2	64	250	2088	250
WS_519CE0211	86	0.006	1.0	7.5	7.7	515.0	0.26	0.17	1.1	2	2	3292	150
WS_505PS0174	50	0.018	1.5	11.3	8.1	3.3	0.20	0.21	1.2	445	5000	50	250
WS_519PS0340	48	0.009	0.7	6.7	10.3	335.0	0.29	0.29	1.3	2	90	2245	150
WS_526PS0764	88	0.085	1.3	11.0	8.6	1.3	0.17	0.40	1.1	1000	2500	647	250

## Supplementary Material References

- Anderson MJ. 2001. A new method for non-parametric multivariate analysis of variance. *Austral Ecology* 26: 32–46. DOI: 10.1111/j.1442-9993.2001.01070.pp.x [online] Available from: <http://onlinelibrary.wiley.com/doi/10.1111/j.1442-9993.2001.01070.pp.x/abstract> (Accessed 10 October 2017)
- Clarke KR. 1993. Non-parametric multivariate analyses of changes in community structure. *Australian Journal of Ecology* 18: 117–143. DOI: 10.1111/j.1442-9993.1993.tb00438.x [online] Available from: <http://onlinelibrary.wiley.com/doi/10.1111/j.1442-9993.1993.tb00438.x/abstract> (Accessed 10 October 2017)
- Kammel LE, Pasternack GB, Massa DA, Bratovich PM. 2016. Near-census ecohydraulics bioverification of *Oncorhynchus mykiss* spawning microhabitat preferences. *Journal of Ecohydraulics* 1: 62–78. DOI: 10.1080/24705357.2016.1237264 [online] Available from: <https://www.tandfonline.com/doi/full/10.1080/24705357.2016.1237264> (Accessed 10 September 2018)
- Kasprak A et al. 2016. The Blurred Line between Form and Process: A Comparison of Stream Channel Classification Frameworks. *PLOS ONE* 11: e0150293. DOI: 10.1371/journal.pone.0150293 [online] Available from: <http://journals.plos.org/plosone/article?id=10.1371/journal.pone.0150293> (Accessed 25 January 2018)
- Kruskal JB. 1964. Multidimensional scaling by optimizing goodness of fit to a nonmetric hypothesis. *Psychometrika* 29: 1–27. DOI: 10.1007/BF02289565 [online] Available from: <https://link.springer.com/article/10.1007/BF02289565> (Accessed 7 February 2018)
- Lane BA, Pasternack GB, Dahlke HE, Sandoval-Solis S. 2017. The role of topographic variability in river channel classification. *Progress in Physical Geography* : 0309133317718133. DOI: 10.1177/0309133317718133 [online] Available from: <http://dx.doi.org/10.1177/0309133317718133> (Accessed 22 August 2017)
- Lane BA, Pasternack GB, Sandoval-Solis S. 2018a. Integrated analysis of flow, form, and function for river management and design testing. *Ecohydrology* DOI: 10.1002/eco.1969 [online] Available from: <https://onlinelibrary.wiley.com/doi/abs/10.1002/eco.1969> (Accessed 9 April 2018)
- Lane BA, Sandoval-Solis S, Stein ED, Yarnell SM, Pasternack GB, Dahlke HE. 2018b. Beyond Metrics? The Role of Hydrologic Baseline Archetypes in Environmental Water Management. *Environmental Management* DOI: 10.1007/s00267-018-1077-7 [online] Available from: <http://link.springer.com/10.1007/s00267-018-1077-7> (Accessed 2 July 2018)
- Montgomery DR, Buffington JM. 1997. Channel-reach morphology in mountain drainage basins. *Geological Society of America Bulletin* 109 : 596–611. [online] Available from: <http://gsabulletin.gsapubs.org/content/109/5/596.short> (Accessed 28 August 2017)
- Oksanen J, Blanchet FG, Kindt R, Legendre P, Minchin PR, O'hara RB, Simpson GL, Solymos P, Stevens MHH, Wagner H. 2019. *Vegan: Community ecology package* [online] Available from: <https://CRAN.R-project.org/package=vegan>
- Parrett C, Veilleux A, Stedinger JR, Barth NA, Knifong DL, Ferris JC. 2011. Regional skew for California, and flood frequency for selected sites in the Sacramento-San Joaquin River Basin, based on data through water year 2006. U. S. Geological Survey

Poff NL et al. 2010. The ecological limits of hydrologic alteration (ELOHA): A new framework for developing regional environmental flow standards. *Freshwater Biology* 55: 147–170. [online] Available from: <http://onlinelibrary.wiley.com/doi/10.1111/j.1365-2427.2009.02204.x/full> (Accessed 17 August 2016)

Rosgen DL. 1994. A classification of natural rivers. *CATENA* 22: 169–199. DOI: 10.1016/0341-8162(94)90001-9 [online] Available from: <http://www.sciencedirect.com/science/article/pii/S0341816294900019> (Accessed 28 August 2017)

Rosgen DL. 1996. Applied river morphology. *Wildland Hydrology*: Pagosa Springs.

Sutfin NA, Shaw JR, Wohl EE, Cooper DJ. 2014. A geomorphic classification of ephemeral channels in a mountainous, arid region, southwestern Arizona, USA. *Geomorphology* 221: 164–175. DOI: 10.1016/j.geomorph.2014.06.005 [online] Available from: <http://www.sciencedirect.com/science/article/pii/S0169555X14003031> (Accessed 27 January 2018)